Identification of Novel Mutations and their Functional Roles of the Human *ATP7B* Gene in Korean Patients with Wilson Disease

Sangwook Park

Department of Biomedical
Laboratory Science
The Graduate School
Yonsei University

Identification of Novel Mutations and their Functional Roles of the Human *ATP7B* Gene in Korean Patients with Wilson Disease

A Dissertation

Submitted to the Department of Biomedical

Laboratory Science and the Graduate School of

Yonsei University

in partial fulfillment of the

requirements for the degree of

Doctor of Philosophy

Sangwook Park

July 2005

This certifies that the dissertation of Sangwook Park is approved.

Thesis Supervisor:	Jong Bae Kim
Ok Doo Awh:	Thesis Committee Member
Yong Serk Park:	Thesis Committee Member
Hyeyoung Lee:	Thesis Committee Member
Han-Wook Yoo:	Thesis Committee Member

The Graduate School

Yonsei University

July 2005

This dissertation is affectionately dedicated to my parents,

my sister, my brothers, my wife and lovely my son,

who have encouraged me.

CONTENTS

LIST OF FIGURES

LIST OF TABLES

ABSTRACT

Identification of Novel Mutations and their Functional Roles of the Human *ATP7B* Gene in Korean Patients with Wilson Disease

Wilson disease (WND), an autosomal recessive disorder of copper transport, is characterized by excessive accumulation of intracellular copper in the liver and extrahepatic tissues. Due to the impaired biliary copper excretion and disturbed incorporation of copper into the ceruloplasmin, hepatic cirrhosis and neuronal degeneration are major symptoms in WND. The *ATP7B*, identified as the gene responsible for WND, has 21 exons and encodes 165 kDa copper transporting P-type ATPase. Screening of *ATP7B* mutation was performed in Korean patients with WND. Among the 125 unrelated Korean patients with WND, thirty different mutations were identified, including p.R778L, p.A874V, p.N1270S, c.2513delA, p.T1029I, p.G1035V, p.L1083F, c.2630_2656del, c.2304_2305insC, p.R919G, p.V1106I, p.D1267A, p.C108R, p.E412X, p.C656X, p.M729V, p.R778Q, p.G891D, p.I929V, p.G943S, p.P992L, p.V1024A, p.T1031A, p.C1091Y, p.I1148T, p.A1168S,

p.G1186S, p.V1216M, p.P1273L and c.1543+1 G>T and ten novel mutations were identified. In order to evaluate the functional defects of ATP7B protein caused by novel mutations, yeast complementation system and confocal microscope were used for analyzing the localization of mutants after transient expression in mammalian cell system. Five novel mutations, p.C656X, p.G891D, p.V1106I, p.T1029I, and p.T1031A were constructed into the yeast expression vector, pSY114 and the mammalian expression vector, pEGFPC1. Three novel mutant, p.C656X, T.1029I and p.T1031A, were unable to rescue the ⊿ccc2 mutant yeast due to the reduced affinity iron uptake in the yeast complementation system, indicating their defective ATP7B function. A novel mutation found in a patient with less severe symptom, p.G891D partially restored ⊿ccc2 mutant yeast. A p.V1106I was completely restored as wild type which suggested p.V1106I was not a mutation, but a polymorphism. In the trafficking of the mutant ATP7B with confocal microscope, the mutant p.C656X was dispersedly throughout transfected COS-7 cells. The mutant p.G891D was partially localized to the site of the *trans*-Golgi network. Two mutants, p.T1029I and p.T1031A were predominantly mislocalized to perinuclear regions. A mutant p.V1106I was normally targeted to the *trans*-Golgi network, which was concordant with the result in the yeast complementation system. In characterizing functional defects of ATP7B and correlate genotype-phenotype in patients with WND,

yeast complementation system and confocal microscopic evaluation were useful tools for functional study on mutant ATP7B protein.

Keywords: Wilson disease (WND), ATP7B, yeast complementation system, confocal microscope

CHAPTER I

Identification of genetic mutations in the human *ATP7B* gene of Korean patients with Wilson disease

I. INTRODUCTION

Wilson disease (WND; OMIM: #277900), an autosomal recessive disorder of copper transport, is characterized by excessive accumulation of intracellular copper in the liver and extrahepatic tissues resulting from impaired biliary copper excretion and disturbed incorporation of copper into the ceruloplasmin (Scheinberg IH *et al.*, 1984).

Although sporadic reports of a similar clinical syndrome appeared in the literature as early as 1850, WND was recognized as a distinct entity in 1912 by Samuel Alexander Kinnear Wilson, who reported several cases of a new familial disorder resulting in progressive degeneration of the lenticular nuclei invariably associated with hepatic cirrhosis at autopsy (Wilson SAK, 1912). The WND gene, *ATP7B*, identified as the gene responsible for this disease, has 21 exons spanning more than 60 kb on chromosome 13q14.3 and encodes the 165 kDa copper transporting P-type ATPase (Petrukhin K *et al.*, 1994). *ATP7B* gene was cloned and shown to encode a member of family of cation-transporting P-type ATPases in 1993 (Yamaguchi Y *et al.*, 1993; Bull PC *et al.*, 1993; Tanzi RE *et al.*, 1993). The *ATP7B* gene was isolated and fully characterized in 1994 (Wu J *et al.*, 1994).

Copper is an essential trace metal, utilized as a cofactor by numerous enzymes regulating vital cellular functions, including cellular respiration, oxidative phosphorylation, pigment formation, neurotransmitter biosynthesis,

radical detoxification, iron uptake and connective tissue formation (Culotta VC *et al.*, 2001). The importance of copper for normal cell metabolism is best illustrated by the existence of severe genetic disorders, in which the normal distribution of copper is disrupted. The copper-transporting ATPase, ATP7B, plays an essential role in removing excess copper from human body by transporting copper from the liver to the bile. Mutations of *ATP7B* lead to vast accumulation of copper in the liver, brain and kidneys, causing a set of pathological symptoms, known as Wilson disease. Severe liver lesions, neurological problems and a wide spectrum of psychiatric abnormalities are common symptoms of WND. Although little known about their precise mechanisms of copper excretion and physiologic functions, identification of causative mutations in WND patients has been carried out in European and Northern American patients for confirmation of the clinical diagnosis, enabling presymtomatic recognition of affected sibs of a definite patients. In Asian populations, mutation reports have been described in Japanese, Taiwanese and Chinese with WND patients (Liu XQ *et al.*, 2004; Okada T *et al.*, 2000; Tsai CH *et al.*, 1998). The age of onset of WND patients vary widely as well as clinical presentation and no exact incidence has been determined in Korea.

Analysis of the derived amino acid sequence from the *ATP7B* revealed a membrane protein predicted to transport copper across the lipid bilayer in an

ATP-dependent manner. A homologous copper-transporting P-type ATPase has been identified in a wide variety of prokaryotic and eukaryotic species (Lutsenko S *et al.*, 1995; Solioz M *et al.*, 1996). The ATP7B contains a number of amino acid motifs; MXCXXC, CPC, ITGEA, DKTGT, GDGVND and SEHPL sequences, characteristic of such ATPases including MXCXXC copper-binding sequences in the N-terminus, a transmembrane CPC that is essential for metal transfer across the membrane, an ITGEA phosphatase domain, a conserved DKTGT sequence that is the site of the aspartyl-phosphate intermediate (acylphosphate) essential for energy transduction, and a GDGVND motif forming the ATP-binding domain and a highly conserved sequence, SEHPL, is found proximal to the ATP-binding domain.

Analysis of mutations in patients with WND reveals an enormous heterogeneity, consisting of a very small number of frequent mutations that are specific in the population, as well as a much greater number of rare individual alleles. To date, almost 270 different mutations have been described in WND patients from varying ethnic origins (Gu YH *et al.*, 2003; Loudianos G *et al.*, 2002; Nanji MS *et al.*, 1997). Of these, more than four-fifths are missense mutations, occurring in transmembrane domains or the ATP-binding region. The remainders of the characterized mutations consist of small deletions/insertions, nonsense mutations, and splicing site abnormalities. Absence of specific mutations in coding regions implies the

presence of mutations in promoter regions controlling transcription of the WND gene (Cullen LM, 2003). Among the common mutations, p.R778L in transmembrane domain 4, has been identified in about 30 percent of the alleles in Asian populations (Chuang LM *et al.*, 1996; Kim EK *et al.*, 1998).

The diverse malfunctions of liver with copper toxicity include variable combinations of acute or chronic hepatitis, cirrhosis, fulminant liver failure, hemolysis, neurological symptoms largely with motional disorder and renal failure (Sherlock S, *et al.*, 1993). When WND patients are untreated, they are usually crippling and frequently fatal in affected individuals, but highly effective therapy is available in the forms of various copper chelator; D-penicillamine, Dihydrochloride (trientine), and alternatively zinc salts (Scheinberg IH *et al.*, 1987; Walshe JM *et al.*, 1982). The goal of treatment in WND is to restore the normal copper homeostasis through systemic chelation therapy by removing or detoxifying accumulated copper in the liver. However, the treatment with those drugs is complicated during his/her lifelong and side effects cannot be tolerated (Sherlock S, *et al.*, 1993). Therefore, liver transplantation is one of the curable treatments, but there is significant morbidity and risk associated with the procedure (Schilsky ML *et al.*, 1994). Wilson disease has worldwide frequency of one in 30,000 with a carrier frequency of one of 90 (Scheinber I *et al.*, 1984). The diagnostic criteria is based on a combination of low serum ceruloplasmin (<20 ㎍/dℓ) and

increased urinary excretion of copper (> 100 μg/day), demonstrating chronic presentation of movemental disorder associated with Kayser-Fleischer (KF) rings with or without cirrhosis. Diagnostic failure of WND can result in lost opportunities for effective copper-chelating therapy and the development of crippling complications. The biochemical laboratory tests may give false positive results in heterozygote carriers. It may result in inappropriate lifelong administration of potentially toxic drugs and genetic stigmatization (Frommer D *et al.*, 1997, Steindl P *et al.*, 1997). Furthermore, the biochemical criteria cannot be applied for prenatal diagnosis because hepatic ceruloplasmin synthesis occurs after birth and is associated with a gradual rise in plasma. Therefore, genetic diagnosis can be substituted to overcome all of these limitations and it may provide prognostic information.

This study aims to identify genetic molecular defects in Korean patients with WND and also is to establish the *in vitro* plating assay based on the yeast complementation. To validate the usefulness of yeast complementation system for routine mutation screening of *ATP7B*, we analyzed *ATP7B* gene with WND and subsequently applied novel mutations or polymorphisms for the yeast complementation assay. The novel mutants were also constructed into mammalian vector system, and then the localization of wild type protein, ATP7B and mutant one was simultaneously examined under a confocal microscope.

II. MATERIALS AND METHODS

Materials

PCR *Taq* DNA polymerase and restriction enzymes were purchased from Promega (Medison, WI, USA). Silver stain solutions were purchased from Bio-Rad (Hercules, CA, USA). BigDye Termination version 3.0 Kit was purchased from United States Biochemical (Cheveland, OH, USA). All other chemicals and solvents were reagent grade.

Subjects

This study was approved by Institutional Review Board (IRB) of Asan Medical Center. All of patients were Korean and underwent clinical examinations. The study included 125 patients from 120 unrelated families, diagnosed on the basis of two biochemical findings; a low serum ceruloplasmin level (<20 ㎎/dℓ) and increased urinary copper excretion (> 100 ㎍/day).

Establishment of lymphoid cell lines

Peripheral blood samples of participating individuals were collected with informed consent from 120 unrelated probands with WND and those family members. Lymphoid cell lines were established using cyclosporine A and

Epstein-Barr virus (EBV).

Genomic DNA isolation

Genomic DNA was extracted from peripheral blood leukocytes of patients or EBV immortalized cell lines. Specimens were centrifuged at 1,300 g for 10 minutes and the supernatant plasma was discarded. After the pellets suspended with 0.5% sodium dodecyl sulfate, proteinase K was added to a final concentration of 100 ㎍/㎖ and then the mixture was placed on a water bath for 3 hours at 50℃. After the reaction was completed, genomic DNA was extracted with phenol, chloroform and isoamylalcohol (25:24:1) and centrifuged 12,000 g for 10 minutes. Subsequently, genomic DNA was precipitated with 99.9% pure ethanol, and the precipitated genomic DNA was washed twice with 70% ethanol. Finally, the genomic DNA was briefly dried and resuspended with TE buffer (10 mM Tris·Cl; 1 mM EDTA, pH 8.0). The purity and concentration of DNA was determined by measuring of absorbance at 260 nm/280 nm. (Aldridge J *et al.,* 1984) using a Spectrophotometer (NonoDrop-1000, Wilmington, USA).

Polymerase chain reaction (PCR)

The amplification for all of 21 coding exons and flanking intronic regions of *ATP7B* gene was performed with 21 pairs of synthetic oligonucleotide

primers (Table I-1) designed to cover all of the exons and their proximal intergenic sequences. The amplification was performed in 30 cycles, each cycle consisting of denaturation at 95℃ for 30 seconds, annealing at 60℃ for 30 seconds, and extension at 72℃ for 35 seconds. PCR was carried out in reaction volumes of 20 ㎕ in a thermocycler, GeneAmp® PCR System 9700 (Applied Biosystems, USA), containing 100 ng of genomic DNA template, 0.5 uM each of primers, 200 uM each of dNTPs, 1.5 mM $MgCl_2$, 10 X buffer [50 mM KCl, 10 mM Tris-HCl (pH 9.0 at 25℃), 50 mM KCl and 0.1% Triton® X-100]] and 1.0 unit of *Taq* polymerase.

Table I-1. Sequences of oligonucleotide primers used for amplification of *ATP7B* gene

Exon	Primer Sequence (5´→3´)		Size of Amplicon (bp)
	Forward	Reverse	
1	TTCCCGGACCCCTGTTTGCT	AATCCTCCTGGTGGGAGTGAGCAC	274
2a	GTTTCAAGGTTAAAAAATGT	GGCACATATTTCACAGTGG	392
2b	GGCCACCAGCAC AGTC	CTGGGCAGGCAAGGAC	402
2c	GAGGCCAGCATTGCAGA	AGCCACTTTGCTCTTGATG	406
2d	GCCCAAGTAAAGTATGACCC	GACACCGATATTTGCTGCAC	311
2e	GGCACATGCAG ACCACTCT	GGCTCACCTATACCACCATCC	301
3	ATATTTTCTGACATTTTATCC	GCAGCATTCCTAAGTTCA	427
4	CCACCCAGAGTGTTACAGCC	ACCCCGTAACGCACCCA	390
5	CCTGGGTCTGTGGGATTCT	AAAGGTGACTACAATTTTTTAATG	357
6	CTGCCAATGCATATTTTAAC	GGTAGAGGAAGGGACTTAGA	278
7	TGTAATCCAGGTGACAAGCAG	CACAGCATGGAAGGGAGAG	380
8	CAGCCTTCATGTCCTTGTC	GAGCAGCTCTTTTCTGAAC	369
9	TTTCGATAGCTCTCATTTCACA	TGCCCACACTCACAAGGTC	321
10	AGTGGCCATGTGAGTGATAA	CTGAGGGAACATGAAACAA	289
11	CTGTCAGGTCACATGAGTGC	TTTCCCAGAACTCTTCACA	347
12	CTTGTGGTGTTTTATTTCTTC	ACCACCATATAGCCCAAG	364

Table I-1 (Continued)

Exon	Primer Sequence (5´→3´)		Size of Amplicon (bp)
	Forward	Reverse	
13	TGAACTCTCAACCTGCCT	TCAGGATGGGGAAAGCCG	378
14	TCCATCTGTATTGTGGTCAG	CAGCTAGGAGAGAAGGACAT	345
15	CTTTCACTTCACCCCTCT	CAGCTGCAGAGACAAAAGC	385
16	CCATTTAGAAATAACCACAG	AGGAAGGCAGAAGCAGA	362
17	CAAGTGTGGTATCTTGGTG	CTGGTGCTTACTTTTGTCTC	357
18	ACCTTTTGCCAACACTAGGCA	TCCCAGCACCCACAGCC	345
19	GGCAGACCCCTTCCTCAC	CCTGGGAGACAGAAGCCTTT	334
20	CTAGGTGTGAGTGCGAGTT	CAGCATTTGTCCCAGGT	317
21	AATGGCTCAGATGCTGTT	GCTTGTGGTGAGTGG AGG	407

Single-strand conformational polymorphism (SSCP) analysis

Primer pairs to the 5 major hot-spot exons (exon 8, 10, 11, 15, 18) were tested for PCR amplification and polymorphic genotypes on SSCP gels. Four-microliter of PCR amplicon was mixed with the same volume of loading buffer (95% formamide, 20 mM EDTA, 0.05% bromphenol blue, 0.5% xylene cyanol FF) and loaded on 8% non-denaturating polyacrylamide gel. The PCR products were denatured to single-stranded DNA by heating at 95℃ for 5 minutes and immediately cooled on ice. Three-microliter of this mixture was separated on 8% non-denaturating polyacrylamide, 100 × 80 × 0.75 mm SSCP gels with a mutation detection gel solution. The gel mixture was prepared in a 5 ㎖ total volume, containing a final concentration of 8% acrylamide /bisacrylamide solution (29:1), 20% glycerol and 1.0 × TBE buffer and polymerized by adding the 20 ㎕ of 10% ammonium persulphate and 3 ㎕ of tetramethylenediamine (TEMED). Fragments were subjected to electrophoresis for 3 hours at a constant power of 200 V and 40 ㎃ at 4℃ in a water cooler apparatus and then silver stained according to the manufacturer's recommended methods (Amersham, Genephore, USA).

Direct sequencing of double stranded PCR products

When a mobility shift band was detected by the single-stranded conformational polymorphism (SSCP) analysis, the PCR product was

subsequently utilized for direct double-stranded DNA sequencing with the same primers used in PCR reaction and a BigDye Termination version 3.0 kit (ABI system, Forster, USA) according to the manufacturer's instructions with following modifications. The amount of template for each sequencing reaction ranged from 0.1 to 0.5 ㎕ of each PCR products and 1.0 uM each of primers. The BigDye was diluted eight volumes with enzyme dilution buffer (400 mM Tris·Cl; 10 mM $MgCl_2$, pH 9.0). After the reaction was completed, the reactant was subjected to electrophoresis on ABI 3100 Genetic Analyzer (ABI system, Forster, CA, USA) with POP6 polymer as running matrix. Chromatographic results of sequences were analyzed by a computational software ABI PRISM Sequence Analysis version 3.7 (ABI system, Forster city, CA, USA).

Restriction fragment length polymorphism (RFLP) analysis

Novel mutations were amplified using modified PCR primers and subsequently, 5 ㎕ of the PCR amplicon was digested with a restriction endonuclease (Table I-2) in a total volume of 10 ㎕ at 37℃ for 1 hour 30 minutes to monitor the mutations in WND patients. Electrophoresis was carried out with 5 ㎕ of the digested DNA on 10% native polyacrylamide gels. The mobility shift bands were visualized using ethidium bromide (10 ㎎/㎖) under a U.V. transilluminator.

Table I-2. Primer pairs used for PCR-RFLP analysis

Novel mutant	Enzyme	[a] Primer synthesis for restriction enzyme site	
p.M729V	*Apa*L I	Sense	GGT CTC ACA TGC TCT TGG TC
		Antisense	AGG ACG ATG AGC ACG T***G***C A
p.G891D	*Sal* I	Sense	CAT TAA AGC TAC CCA CGT ***C***G
		Antisense	TTT CCC AGA ACT CTT CAC A
p.I929V	*Taq* I	Sense	CTT GTG GTG TTT TAT TTC TTC
		Antisense	CGT CAA AGT TGA CAT GAT G***T***
p.V1024A	*Hha* I	Sense	GTC AAG GTC AAG CCT CAG TG
		Antisense	TGC CAG TCT TGT CAA ACA ***G***C
p.C1091Y	*Hha* I	Sense	CTT TCA CTT CAC CCC TCT
		Antisense	GCA CTG CCT GGA AGT CC***C*** TG
p.T1029I	*Hin*d III	Sense	AGA CTG TGA TGT TTG ACA AG***C*** [b]
		Antisense	CAG CTA GGA GAG AAG GAC AT
p.T1031A	*Internal restriction site : Hha* I		
p.V1106I	*Eco*R V	Sense	GCT GTG GAA TTG GGT GC***G*** A***T***
		Antisense	CAG CTG CAG AGA CAA AAG C

[a] All of primers are given in 5′ to 3′ directions.

[b] *Italic* bold basepairs are for creation of a new endonuclease restriction site within the PCR products.

III. RESULTS

Polymerase chain reaction of the *ATP7B* gene in Korean patients with Wilson disease

Twenty one exons and their intergenic sequences were PCR-amplified with 25 sets of primers (Fig. I-1). Subsequently, The PCR products were subjected to electrophoresis on 1.5% agarose gel to examine whether the targeted template was specifically amplified. When a single band was amplified, the PCR products were subsequently utilized as a template for direct double stranded DNA sequencing.

Identification of the candidate novel mutations of the *ATP7B* gene in Korean patients with Wilson disease

DNA sequencing of PCR product was performed in both directions using forward and reverse PCR primers using the same primers for PCR analysis. Thirty different mutations were identified in 125 subjects from 120 unrelated Korean patients with WND. Ten different mutations, involved in evolutionarily conserved nucleotide sequences over species, have not been previously described: c.1234G>T (p.E412X), c.1968C>A (p.C656X), c.2185A>G (p.M729V), c.2672G>A (p.G891D), c.2785A>G (p.I929V), c.3071T>C (p.V1024A), c.3086C>T (p.T1029I), c.3091A>G (p.T1031A),

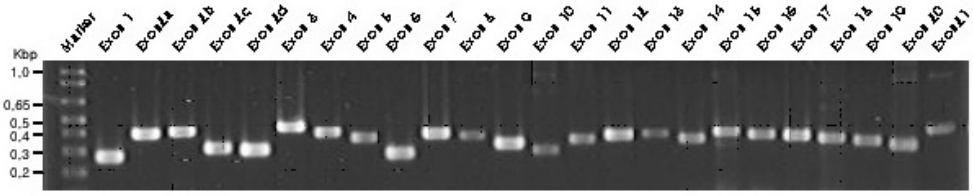

Figure I-1. PCR amplification of the human *ATP7B* gene.

Genomic DNA regions spanning all exons and adjacent introns were amplified, and electrophoresed on 1.5% agarose gel. The 100 bp DNA ladder (Promega, Madison, USA) was used as a size marker. All lanes represent each exon.

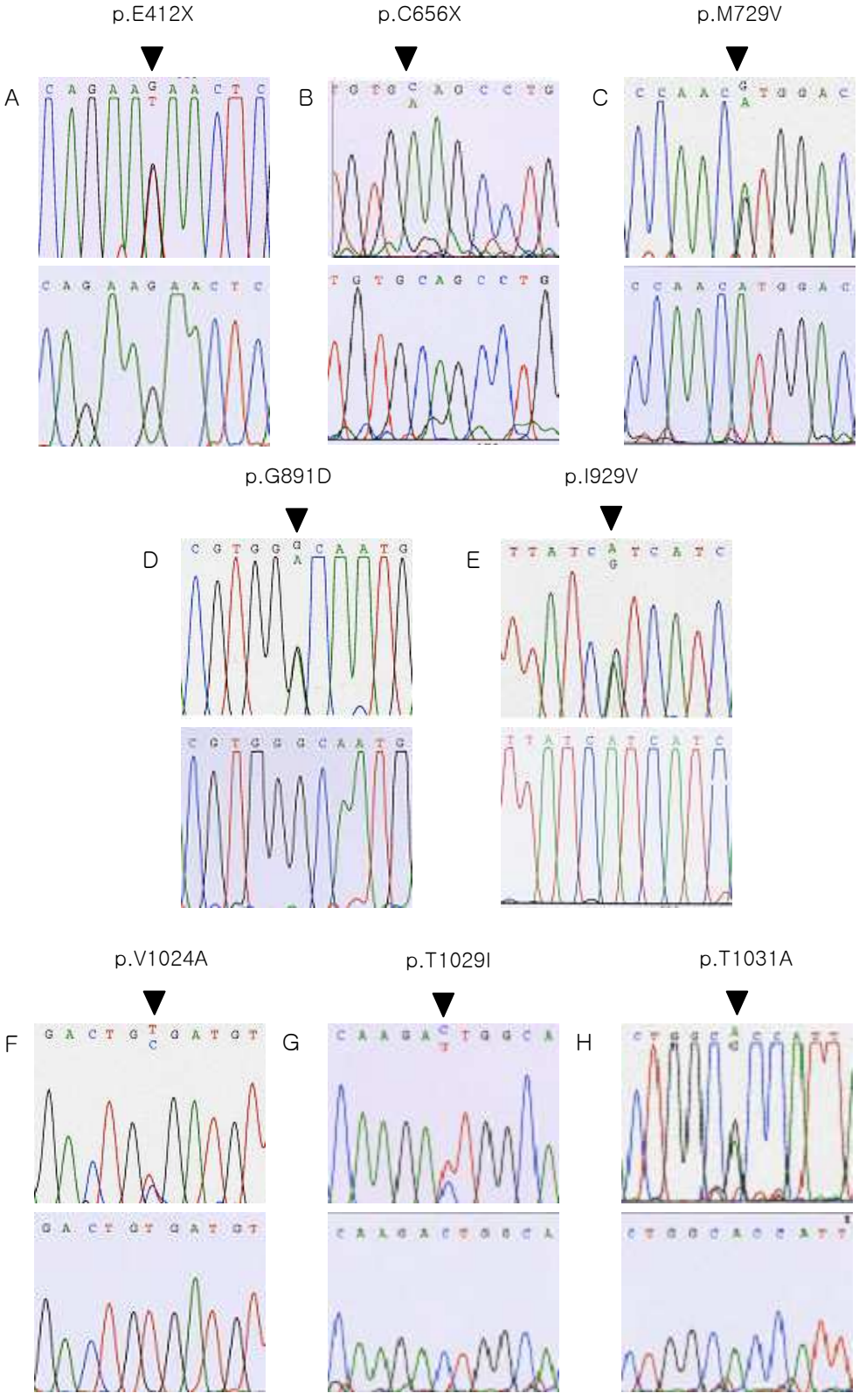
p.E412X
p.C656X
p.M729V
A
B
C
p.G891D
p.I929V
D
E
p.V1024A
p.T1029I
p.T1031A
F
G
H

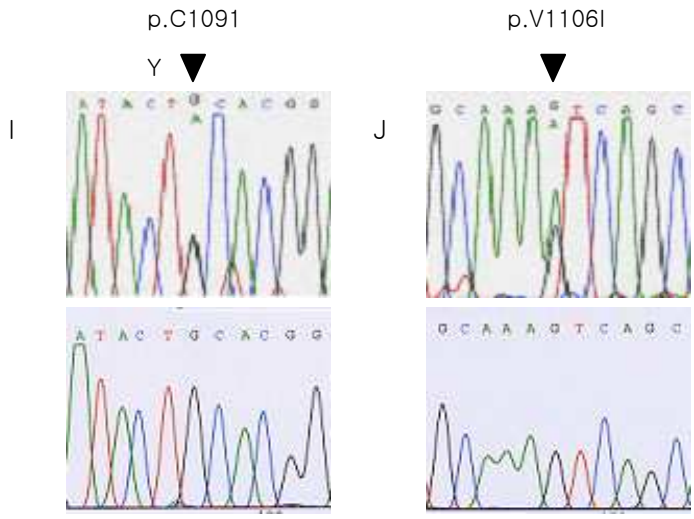

Figure I-2. Identification of novel mutations in the *ATP7B* gene with Wilson disease.

Partial genomic DNA sequence showed novel mutations of the *ATP7B* gene. Capillary electrophoresis was performed in ABI3100 Genetic Analyzer with BigDye terminator version 3.0 Kit. Arrowheads indicate a nucleotide substitution. The novel mutations are following as A; p.E412X, B; p.C656X, C; p.M729V, D; p.G891D, E; p.I929V, F; p.V1024A, G; p.T1029I, H; p.T1031A, I; p.C1091Y and J; p.V1106I.

c.3272G>A (p.C1091Y) and c.3316G>A (p.V1106I) (Fig. I-2). On the other hand, twenty other mutations were previously reported in other studies: c.2333G>T (p.R778L) (Thomas *et al.*, 1995), c.2621C>T (p.A874V) (Yamaguchi *et al.*,1998), c.3809A>G (p.N1270S) (Tanzi *et al.*,1993), c.2513delA (p.L838SfsX34), c.3104G>T (p.G1035V) (Nanji *et al.*, 1997), c.3247C>T (p.L1083F) (Kim *et al.*, 1998), c.1543+1 G>T (IVS3+1 G>T) (Loudianos *et al.*,1998), c.2304_2305insC (p.M769HfsX25) (Figus *et al.*, 1995), c.2630_2656del (p.I877_I885del) (Yamaguchi et al., 1998) in frame deletion, c.2755C>G (p.R919G) (Yamaguchi *et al.*,1998), c.3800A>C (p.D1267A) (Yamaguchi et al., 1998), c.322T>C (p.C108R), c.2333G>A (p.R778Q) (Chuang *et al.*,1996), c.2827G>A (p.G943S) (Thomas GR et al., 1995), c.2975C>T (p.P992L) (Nanji *et al.*, 1997), c.3443T>C (p.I1148T) (Loudianos *et al.*,1998), c.3502G>T (p.A1168S) (Yoo, 2002), c.3556G>A (p.G1186S) (Yamaguchi *et al.*, 1998), c.3646G>A (p.V1216M) (Loudianos *et al.*, 1998) and c.3818C>T (p.P1273L) (Loudianos *et al.*, 1996).

The rate of mutation detected was 75.6% (189/250) by direct sequence analysis of all exons amplified from *ATP7B* gene of the 125 patients. A total of 30 different mutations were found across 21 exons or adjacent introns. Among them, 20 mutations have been reported previously, while ten were candidate novel mutations, consisting of 8 missense mutations, 2 nonsense mutations (Table I-3). Since the variations were not observed in any of the

Table I-3.Novel mutations identified in the human *ATP7B* gene

Exon	cDNA Nucleotide change	Protein codon change	Affected protein domain
2	c.1234G>T	p.E412X [a)]	Cu binding
7	c.1968C>A	p.C656X [a)]	Tm1 [b)]
8	c.2185A>G	p.M729V	Tm4 [b)]
11	c.2672G>A	p.G891D	Td [c)]
12	c.2785A>G	p.I929V	Tm5 [b)]
14	c.3071T>C	p.V1024A	ATP loop
14	c.3086C>T	p.T1029I	ATP loop
14	c.3091A>G	p.T1031A	ATP loop
15	c.3272G>A	p.C1091Y	ATP loop
15	c.3316G>A	p.V1106I	ATP loop

[a)] Allele frequencies in healthy Korean population were not determined since they would result in generation of truncated proteins. Functional domains are as described. [b)] Tm; transmembrane, [c)] Td; transduction.

50 healthy Korean individuals, the 10 novel mutations were not polymorphisms. Four different mutations in exon 8 were found in 41.2% of alleles, three different mutations in exon 11 were found in 9.6% of alleles and three different mutations in exon 18 were found in 7.6% of alleles, thereby indicating that exons 8, 11 and 18 are three important exons for detecting mutations in Korean patients with WND. In particular, the p.R778L mutation in exon 8 was found in 39.6% of these Korean patients in at least one allele. Twenty-four patients with WND were homozygotes for p.R778L and 51 patients with WND were heterozygotes for p.R778L.

In exon 2, p.C108R and p.E412X mutations were identified. A T-to-C (TGC-to-CGC) transversion of the 108th codon of the *ATP7B* gene (p.C108R) induced an amino acid change to arginine. A G-to-T (GAA-to-TAA) transversion of 412th codon resulted in a glutamic acid to a termination codon change.

Between exon 3 and juxtaintronic sequence, a mutation of splicing donor site, c.1543+1G>T was identified. This aberrant splicing mutation will give rise to a difficulty in formation of a lariat for normal splicing.

In exon 7, p.C656X mutation was identified as novel. The p.C656X mutation was C-to-A (TGC-to-TGA) transversion that resulted in a substitution of a stop codon for a 656th cysteine.

In exon 8, mutations of p.R778L, p.R778Q, p.M729V and

c.2304_2305insC were identified. A p.R778L mutation was a G-to-T (CGG-to-CTG) transversion that resulted in a substitution of leucine for 778th arginine. A p.R778Q mutation was a G-to-A (CGG-to-CAG) transition that converted 778th arginine to glutamine. A p.M729V mutation was a A-to-G (ATG-to-GTG) transition that resulted in 729th methione to valine. An insertion C between c.2304 and c.2305 nucleotide was identified. The mutation caused a frameshift leading to termination at 25th codon.

In exon 10, an insertion A mutation, c.2513delA resulted a deletion of 838th amino acid, causing a frameshift from 838th amino acid, and led to a termination at 872th codon.

In exon 11, p.A874V, p.G891D and c.2630_2656del mutations were identified. A p.A874V mutation caused by a C-to-T transition at 84th codon (GCG-to-GTG) converted an amino acid arginine to valine. A p.G891D mutation, which is a G-to-A transition at 891th codon (GGC-to-GAC), converted an amino acid glycine to aspartic acid. A 27 bp in-frame deletion mutation, c.2630_2656del induced an in-frame deletion of 877th-885th amino acid.

In exon 12, p.R919G, p.I929V and p.G943S mutations were identified. A p.R919G mutation caused by a C-to-G transversion at 919th codon (CGG-to-GGG) induced an amino acid arginine to valine. A p.I929V mutation caused by a A-to-G transition at 929th codon (ATC-to GTC) converted an amino acid

isoleucine to valine. A p.G943S mutation caused by a G-to-A transition at 943th codon (GGT-to-AGT) converted an amino acid glycine to serine.

In exon 13, A p.P992L mutation was identified. A p.P992L mutation caused by a C-to-T transition at 992th codon (CCC-to-CTC) converted an amino acid proline to leucine.

In exon 14, mutations were identified with the p.G1035V, p.T1029I, p.T1031A, and p.T1024A. A p.G1035V mutation was a G-to-T (GGC-to-GTC) transversion that converted the 1035th glycine to valine. A p.T1029I mutation was a C-to-T (ACT-to-ATT) transition that converted the 1029th threonine to isoleucine. A p.T1031A mutation was a A-to-G (ACC-to-GCC) transition that induced the 1031th threonine to alanine. A p.V1024A mutation was a T-to-C (GTG-to-GCG) transition that converted the 1024th valine to alanine.

In exon 15, mutations were identified with the p.L1083F, p.V1106I and p.C1091Y. A p.L1083F mutation was a C-to-T (CTT-to-TTT) transition that converted the 1083th leucine to phenylalanine. A p.V1106I mutation was a G-to-A (GTC-to-ATC) transition that converted the 1106th valine to isoleucine. A p.C1091Y mutation was a G-to-A (TGC-to-TAC) transition that induced the 1091th cysteine to tyrosine.

In exon 16, mutations were identified with the pI1148T, p.A1168S and p.G1186S. A p.I1148T mutation was a T-to-C (ATT-to-ACT) transition that

converted the 1148th isoleucine to threonine. A p.A1168S mutation was a G-to-T (GCT-to-TCT) transversion that converted the 1168th alanine to serine. A p.G1186S mutation was a G-to-A (GGT-to-AGT) transition that changed the 1186th glycine to serine.

In exon 17, A c.3577delG mutation was identified. The c.3577delG mutation caused by a deletion of G at 1193th codon followed by a frameshift stop at 1218th codon. A p.V1216M mutation, which was a G-to-A transition at 1216th codon (GTG-to-ATG), converted an amino acid valine to methionine.

In exon 18, mutations were identified with the p.N1270S, p.D1267A, and p.P1273L. The p.N1270S mutation was a A-to-G (AAT-to-AGT) transition that converted the 1270th asparagine to serine. A p.P1267A mutation was a A-to-C (GAT-to-GCT) transversion that converted the 1267th proline to alanine. A p.P1273L mutation was a C-to-T (CCG-to-CTG) transition that induced the 1273th proline to leucine. In summary, there were two nonsense mutations (p.C656X, p.E412X), two small deletion mutations (c.2513delA, c.2630-2656del). There was also a splicing site substitution (c.1543+1 G>T) and a small insertion mutation (c.2304_2305insC). Among all the mutations, 24 mutations were missense (Fig. I-3, Table I-4).

Detection of mobility shift in SSCP

Aberrant migration bands were detected in exon 8 (p.R778L) and exon 18 (p.N1270S), which were hot-spot mutation sites in WND patients in Korea.

It showed strongly that the exon 8 and 18 of *ATP7B* gene might be one of the regions with a higher mutation frequency (Fig. I-4). Although mutation of exon 11 (p.A874V), one of the major mutation sites in this study, was not detected in the SSCP analysis, the p.A874V was elucidated as a major aberrant site in Korean Wilson patients with direct sequencing methods. Of these, mobility shifts were observed with 2304_2305insC in exon 8 (Fig. I-5) and IVS17+6 C>T in exon 18 (Fig. I-6). All of the samples that showed mobility shift bands were subsequently confirmed by direct sequencing methods.

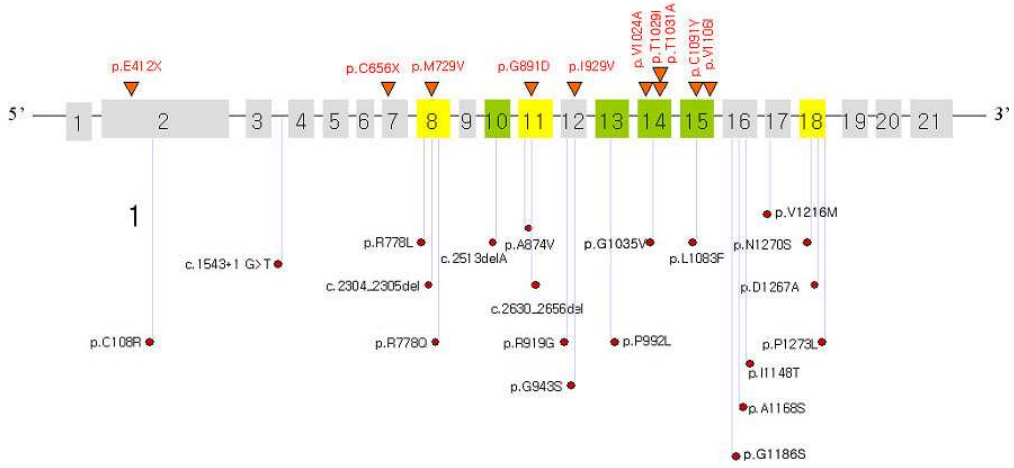

Figure I-3. Locations of mutations identified in the human *ATP7B* gene.

Novel mutations demonstrated on the bar are indicated as coding DNA or affected protein. The novel mutations are shown over the exon bar. The mutations under the exons are shown the reported ones. The p.T1029I and p.T1031A mutations are located in the conserved DKTGT motif that is the essential site for energy transduction.

Table I-4. Distribution of mutations in the human *ATP7B* of Korean Wilson disease patients

Mutation		Exon	Domain	Frequency (%)
Coding DNA	**Affected Protein**			
Missense				
c.2333G>T	p.R778L	8	Tm 4	99 (39.6)
c.2621C>T	p.A874V	11	Td	21 (8.4)
c.3809A>G	p.N1270S	18	ATP hinge	16 (6.4)
c.3086C>T	***p.T1029I***	14	DKTGT motif	5(2.0)
c.3104G>T	p.G1035V	14	ATP loop	5 (2.0)
c.3247G>T	p.L1083F	15	ATP loop	3 (1.2)
c.3556G>A	p.G1186S	16	ATP pocket	3 (1.2)
c.2755C>G	p.R919G	12	Tm5	2 (0.8)
c.3316G>A	***p.V1106I***	15	ATP loop	2 (0.8)
c.3800A>C	p.D1267A	18	ATP hinge	2 (0.8)
c.322T>C	p.C108R	2	Cu 1	1 (0.4)
c.2185A>G	***p.M729V***	8	Tm4	1 (0.4)
c.2333G>A	p.R778Q	8	Tm4	1 (0.4)
c.2672G>A	***p.G891D***	11	Td	1 (0.4)
c.2785A>G	***p.I929V***	12	Tm5	1 (0.4)

Table I-4. (Continued)

Mutation		Exon	Domain	Frequency
Coding DNA	**Affected Protein**			**(%)**
Missense				
c.2827G>A	p.G943S	12	Tm5	1 (0.4)
c.2975C>T	p.P992L	13	Tm6	1 (0.4)
c.3071T>C	***p.V1024A***	14	ATP loop	1 (0.4)
c.3091A>G	***p.T1031A***	14	ATP loop	1 (0.4)
c.3272G>A	***p.C1091Y***	15	ATP loop	1 (0.4)
c.3502G>T	p.A1168S	16	ATP pocket	1 (0.4)
c.3443T>C	p.I1148T	16	ATP pocket	1 (0.4)
c.3646G>A	p.V1216M	17	ATP pocket	1 (0.4)
c.3818C>T	p.P1273L	18	ATP hinge	1 (0.4)
c.3800A>C	p.D1267A	18	ATP hinge	2 (0.8)
Nonsense				
c.2513delA	p.L838SfsX34	10	Td	9 (3.6)
c.1234G>T	***p.E412X***	2	Cu 4	1 (0.4)
c.1968C>A	***p.C656X***	7	Tm1	1 (0.4)

Table I-4 (Continued)

Mutation		Exon	Domain	Frequency (%)
Coding DNA	**Affected Protein**			
Insertion/Deletion				
c.2630-2656del	p.I877_885del	11	Td	2 (0.8)
c.2304-2305insC	p.M769HfsX25	8	Tm4	2 (0.8)
Splice site				
c.1543+1G>T	Intron	Cu5		2 (0.8)
Total				189 (75.6)

Novel mutations are mentioned as a black-bold italic style on the table.

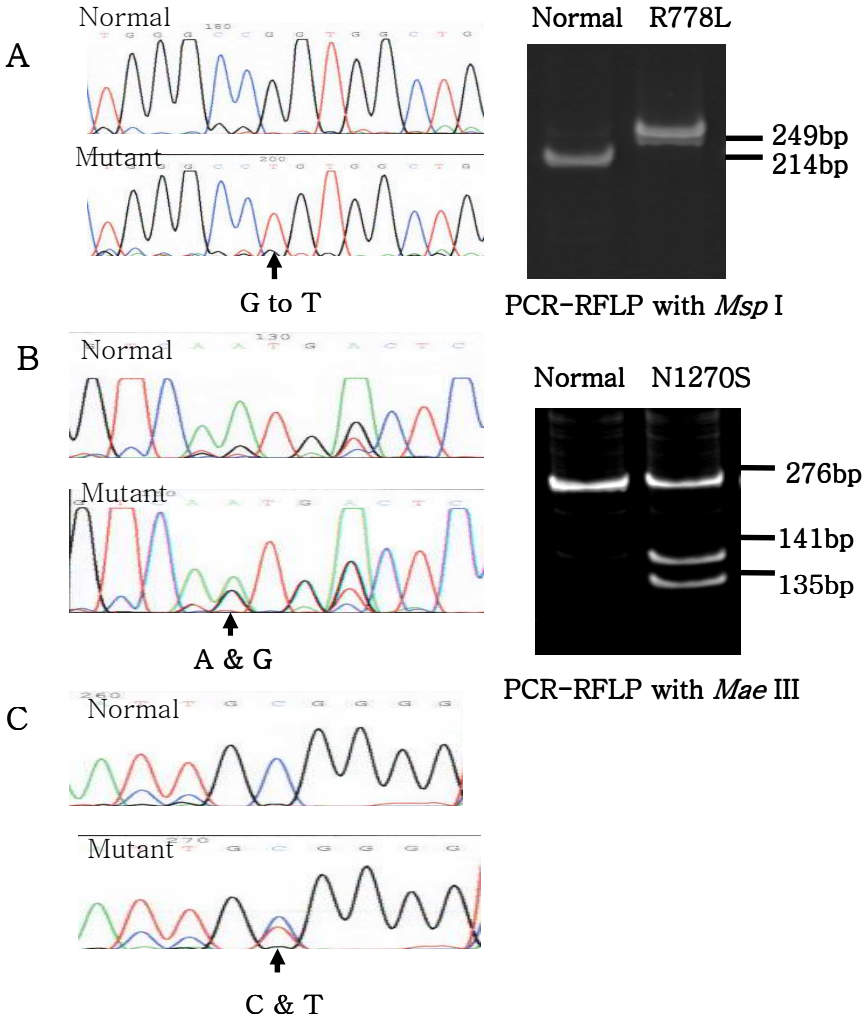

Figure I-4. Three major mutations of human *ATP7B* gene identified in Korean Wilson disease patients.

Partial genomic DNA sequences were obtained with capillary electrophoresis in ABI3100 Genetic analyzer and subsequently digested by two restriction enzymes (*Msp* I, *Mae* III) (A) The p.R778L homozygote was confirmed with *Msp* I. (B) The p.N1270S heterozygote was confirmed with *Mae* III, (C) The p.A874V heterozygote had only direct sequencing data.

오류!

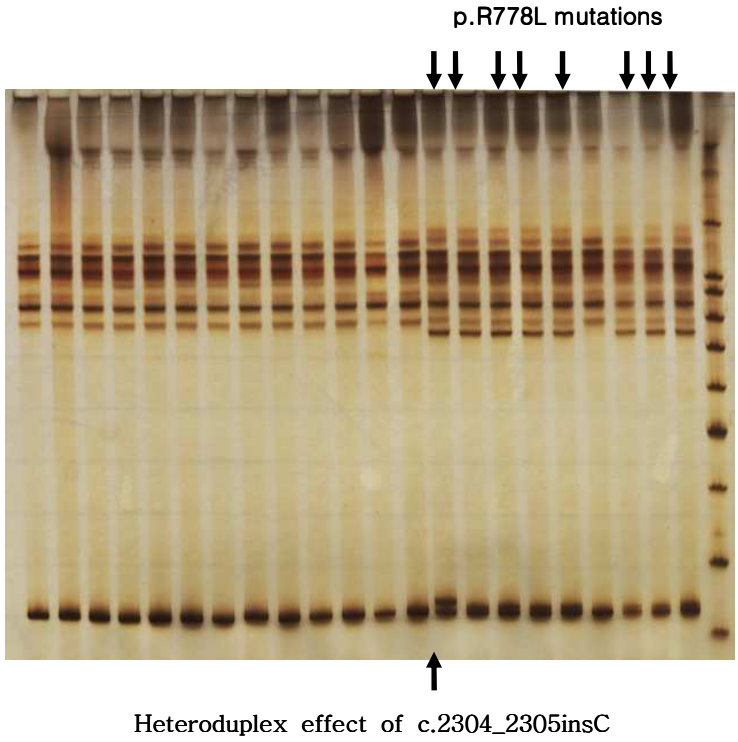

Figure I-5. PCR-SSCP analysis of the p.R778L of the *ATP7B* gene in exon 8.

Downward arrows indicate mobility shifts in the presence of p.R778L mutation. An upward arrow indicates an additional band due to heteroduplex effect.

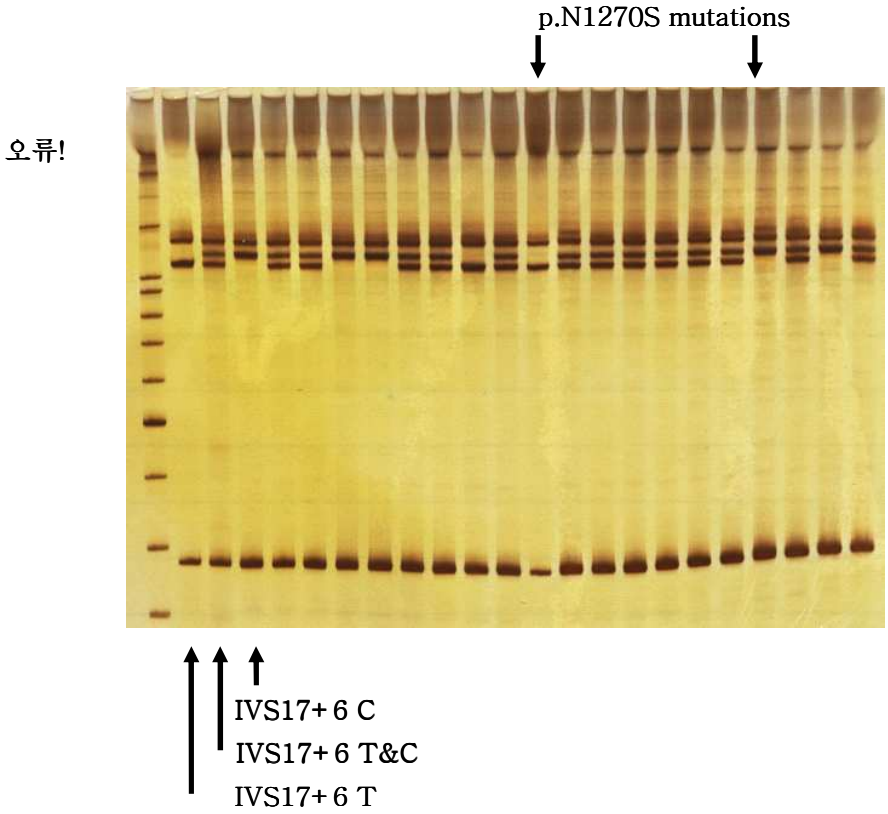

Figure I-6. PCR-SSCP analysis of the p.N1270S of the *ATP7B* gene in exon 18.

Two downward arrows show that mobility band shifts resulting from p.N1270S mutation. Three upward arrows indicate several untypical bands which were resulted from intragenic polymorphisms.

RFLP analysis of novel mutations

In order to exclude the possibility of polymorphism instead of the candidate novel mutations; p.M729V (c.2185 A>G), p.G891D (c.2672 G>A), p.I929V (c.2785 A>G), p.V1024A (c.3071 T>C), p.T1029I (c.3086 C>T), p.T1031A (c.3091 A>G), p.C1091Y (c.3272 G>A) and p.V1106I (c.3316 G>A), the presence of mutations were analyzed by a PCR-RFLP analysis in 50 healthy individuals of Korean populations (Fig. I-7)

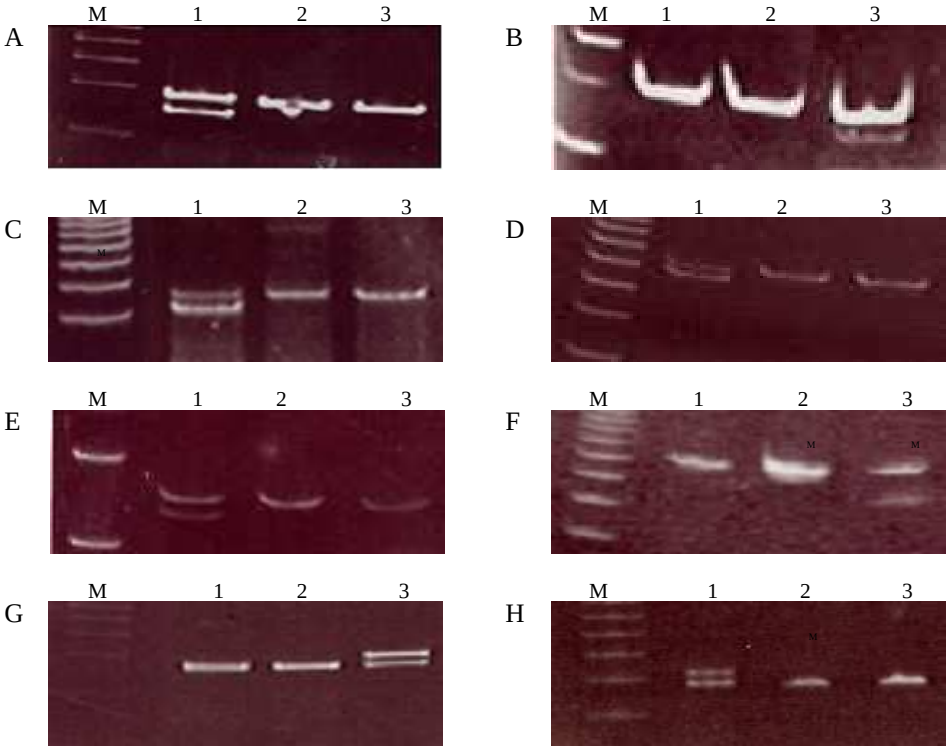

Figure I-7. PCR-RFLP analysis for novel mutations.

Novel mutations modifying endonuclease restriction sites were subjected to electrophoresis on non-denaturating polyacrylamide gel. A: p.M729V with *Apa*L I; B: p.G891D with *Sal* I; C: p.I929V with *Taq* I; D: p.V1024A with *Hha* I; E: p.T1029I with *Hin*d III; F: p.T1031A with *Hha* I; G: p.C1091Y with *Hha* I; H: p.V1106I with *Eco*R V. In figures of A through F, 1: cut for patient (mutant type: heteroduplex), 2: uncut for normal (wild type), 3: PCR product (negative control). In figure of G, 1: cut for normal (wild type), 2 cut for 2nd normal (wild type), 3: uncut for patient (mutant type: heteroduplex). In the figure of H, 1: uncut for patient (mutant type: heteroduplex), 2: cut for normal (wild type), 3: cut for 2nd normal (wild type).

IV. DISCUSSION

A mutation screening of the peripheral *ATP7B* gene in 125 patients by PCR-SSCP analysis following direct sequencing has revealed 30 different mutations, which of them represented ten novel changes. All mutations identified and affected domains were documented (Table I-4).

The p.H1069Q mutation which is the most common WND mutation in eastern and northern European populations, accounting for approximately 30% of the WND chromosomes (Tanzi *et al.*, 1993; Thomas *et al.*, 1995) was not detected. On the other hand, the p.R778L mutations were common in the human *ATP7B* in Korean patients with WND, occurring in more than 40% of these alleles, which meant the p.R778L in the 4^{th} transmembrane domain might reflect a founder effect. The 30 mutations identified in this study accounted for 75.6% of the WND chromosomes screened by PCR-SSCP following a direct sequence analysis. Failure to detect the remaining mutations could be due to the limitation of PCR-SSCP analysis, the experimental conditions used in this study, the presence of mutations in the promoter, introns, and other DNA control regions outside of the exons and their flanking sequences. The normal healthy volunteers were not examined as control subjects in the study. The nonsense mutations, p.E412X in 4^{th} copper binding domain and p.C656X in the first transmembrane domain, most likely resulted in the premature stop codon, leading to produce shortened

protein products or nonsense-mediated truncated protein. The former was found as a compound heterozygote with neurological symptoms, and the latter was also found as a compound heterozygote with the p.R778L mutation. The p.M729V amino acid substitution represented the molecular cause for the hepatopathy with no neurological symptom, which was an mutation in the 4^{th} transmembrane domain except that of p.R778L in the same exon. This observation might be explained by leaky alternative splicing transcripts including some exons (exon 6, 7 and, 8 or only exon 8) in the brain. Since the p.M729V is located in exon 8 and a transcript of the *ATP7B* gene in the brain is lack of exon 8, brain tissues would not be involved in this mutation. However, homozygotes of the p.R778L mutation have been reported to be associated with neurological involvement. The amino acid 729 resides in the 4^{th} transmembrane domain of the protein. The side chain length and polarity of valine are different from those of methionine and may display a steric hindrance in the large transmembrane region, thus a functional loss of the transmembrane helix can be occured.

The p.G891D, detected in exon 11, was a novel mutation and replaced a small nonpolar residue with a larger acidic side chain. It was reported as p.G891V previously at this amino acid in other study (Loudianos *et al.*, 1996) which was located 23 amino acids to the transduction domain in a sequence that was highly conserved in Menkes and other P-type ATPase. Patients with

this mutation showed no clinical symptoms related with WND. Although heterozygotes often function perfectly normally, it is postulated that this is a kind of gain of function mutation, inducing a modified gene to cause a normal phenotype. The p.A874V, detected in exon 11, is the second most common mutation with an allele frequency of 8.4% and replaces a simple nonpolar resudue with a larger one, which is proximal to the phosphatase domain (Giltin *et al.*, 2001). It will presumably disrupt the transduction related domain of the ATP7B protein.

Two mutations, p.T1029I and p.T1031A detected in exon 14 were novel mutations, replacing a hydrophilic residue with a hydrophobic one. Interestingly, these mutations were located in the motif of conserved DKTGT sequence. The mutant p.T1031A was an unknown mutation but other amino acid substitution was reported by other group at the same amino acid position (Duc HH *et al.*, 1998), the mutation of p.T1029I was also considered to be novel, since these aberration was not detected among 100 normal alleles. Patients with this mutation represented neurological symptoms. The highly conserved DKTGT sequence, which was the site of the aspartyl-phosphate intermediate essential for energy transduction might be disrupted from the mutations and no ATP energy dependent copper-transporting ATPase could be definitely expected. Although the substitution of alanine for valine may be negligible subtle change, the p.V1024A is highly proximal to the DKTGT

motif that may provide the causal impairment of energy transduction. The p.V1106I mutation was present in the ATP loop resulting in ATP binding domain which was not also found in 100 alleles in normal population study. This mutation was a conservative region with comparison of the ATP7B orthologue among other species including the paralogue ATP7A (Fig.II-11).

The yeast complementation assay was developed, enhancing the certainty of the significance of amino acid changes in the study. When a functional protein assay is available on the basis of metal-dependent yeast homeostasis, it will be of great advances for DNA diagnostic tests. Wilson disease is a curable disorder when the disease is diagnosed as early as possible. Establishment of an early detection protocol such as the massive screening method will be very helpful for the patients as well as medical practitioners. This study expanded our knowledge on the spectrum of mutations in the *ATP7B* gene in Koran patients and provided new information on critical DNA sequences for the gene function.

CHAPTER II

Functional analysis of the mutant ATP7B protein using yeast complementation assay and confocal microscopy

I. INTRODUCTION

Wilson disease is a genetic disorder of copper metabolism characterized by the toxic accumulation of copper in the liver and in extrahepatic sites. Copper is an essential trace element that permits the facile transfer of electrons in a diverse group of cuproenzymes required for cellular respiration, iron oxidation, pigment formation, neurotransmitter biosynthesis, antioxidant defense, peptide amidation and connective tissue formation. Numerous dietary foods are rich in copper that is absorbed primarily through the stomach and duodenum. Biliary excretion is the only physiological route for copper elimination and each day, an amount of copper is excreted in the bile that is equivalent to that absorbed in the gut (Gitlin JD, 2003).

The liver plays a critical role in copper metabolism, serving as the site of storage for this metal and the primary determinant regulating biliary excretion (Tao TY *et al.*, 2003). Studies using copper isotopes show rapid clearance of this metal from the portal circulation with 10% of the isotope reappearing in the serum bound to the plasma protein ceruloplasmin within 24 hours after a single dose. Ceruloplasmin is a ferroxidase that has an essential role in iron metabolism and contains greater than 95% of the plasma copper. The remaining copper present in the plasma is bound to amino acids, and it is believed that these complexes provide the mechanism for transport

of this metal to various tissues (Hellman NE *et al.*, 2002).

The uptake and storage of copper in the liver occurs in hepatocytes, which determine the rate of biliary excretion of this metal. The essential role of hepatocytes in copper metabolism is shown by the normalization of copper homeostasis in copper-overloaded individuals with WND after liver transplantation (Emre S *et al.*, 2001). At steady state, the amount of copper excreted in the bile is directly proportional to the size of the hepatic copper pool. The normal hepatocyte is capable of rapidly increasing biliary copper excretion in response to systemic copper overload, and therefore, hepatic copper overload is an unusual occurrence under normal physiological conditions (Gollan JL *et al.*, 1973). There is no enterohepatic circulation of copper, and once excreted into the bile, this metal exists as an unabsorbable complex that is excreted in the stool. Ceruloplasmin is synthesized in hepatocytes and secreted into the plasma after the incorporation of copper late in the secretory pathway (Hellman NE *et al.*, 2002). Failure to incorporate copper during ceruloplasmin biosynthesis results in the secretion of an apoprotein that is devoid of enzymatic activity and rapidly degraded (Olivares M *et al.*, 2000).

Wilson disease protein (ATP7B) is a copper-transporting P-type ATPase expressed within the secretory pathway of hepatocytes, and inherited loss-of-function mutations in the gene that encodes this ATPase result in WND

(Schaefer M *et al.*, 1999). ATP7B is predominantly located at the *trans*-Golgi network and functions to transfer copper into the secretory pathway for both incorporatioin into apoceruloplasmin and excretion into the bile (Lutsenko S *et al.*, 2003). As the hepatocyte copper content increases, ATP7B cycles to a cytoplasmic compartment near the canalicular membrane, where copper is accumulated in vesicles before biliary excretion (Schaefer M *et al.*, 1999). In patients with WND, the lack of functional ATP7B limits the copper available for incorporation into ceruloplasmin, resulting in secretion of a rapidly degraded apoprotein. The resulting decrease in serum ceruloplasmin concentration is a diagnostic hallmark of this disorder. Although the cell biological mechanisms of vesicular membrane of hepatocytes are unknown, recent studies in Bedlington terrier copper toxicosis have identified a small cytosolic protein termed *Murr*1 that is required for this process (van De Sluis B et al., 2002). A homologous protein has been detected in human liver suggesting that further analysis of *Murr*1 function will provide useful insights into this pathway of hepatic copper metabolism.

Several motifs found in all P-type ATPases are present in ATP7B, including an invariant aspartate residue that is the site of the β-aspartyl phosphoryl intermediate required for adenosine triphosphate-dependent copper transport across the lipid bilayer (Payne AS *et al.*, 1998). Copper transport requires metal transfer from the amino-terminus to a high-affinity

site in the transmembrane channel, accompanied by adenosine triphosphate binding and aspartate phosphorylation (Moller JV et al., 1996). P-type ATPases defined as the forming a covalent phosphorylated intermediate in their reaction cycle transport a variety of cations across membranes. The general features of those include the TGEA/S motif (phosphatase domain), the DKTGT/S motif (phosphorylation domain), the TGDN motif (ATP-binding domain), and the sequence MXGDGXNDXP that connects the ATP binding domain to the transmembrane segment. ATP7B is further classified as a heavy metal transporting P-type ATPase which pumps copper or cadmium. The six repeated motifs, MXCXXC, at the N-terminus of *ATP7B* are thought to be copper binding domains from their homology with *Cop*A, a copper transporting ATPase in copper resistant strains of *Enterococcus hirae*. The ATP7B also contains the SEHPL and CPC motifs, conserved in heavy metal transporting ATPases and involved in heavy metal translocation. The most common disease allele found in Northern European populations with WND is an H1069Q misense mutation found within a conserved SEHPL motif in the cytoplasmic loop between the fifth and sixth transmembrane domains (Petrukhin K *et al.*, 1994; Thoma GR *et al.*, 1995). This mutation results in a temperature-sensitive defect in ATP7B folding and copper-dependent trafficking, suggesting a potential role for this motif in the intracellular localization of ATP7B .

Copper and iron metabolism in eukaryotic cells have been developed with the baker's yeast *Saccharomyces cerevisiae* (Askwith C *et al.*, 1998; Labbe S *et al.*, 1999). Iron transport in *S. cerevisiae* has revealed a dependence of iron metabolism on adequate copper nutrition and this molecular interaction has provided valuable insight into the basis for the connection between copper and iron nutrition in mammals. The yeast *Ccc2* gene, orthologous to the human Wilson (ATP7B) and Menkes (ATP7A) genes, has been shown to encode a copper transporting P-type ATPase with two copies of the conserved copper binding motif. In yeast *Saccharomyces cerevisiae*, the plasma membrane protein, Ctr1p transports copper into the cytoplasm, in which it is carried by the copper chaperone, Atx1 to Ccc2p. Copper is supplied to Fet3p across the membrane of a *trans*-Golgi compartment (Yuan DS *et al.*, 1997). Fet3p protein, known as a membrane bound ceruloplasmin-like protein in yeast, is required for ferrous transport indispensable for yeast growth. The copper binding to Fet3p is necessary to manifest its oxidase activity. Therefore, Ccc2p is involved in high affinity iron uptake. On the other hand, △ccc2, the yeast mutant strain lacking *Ccc2*, can survive in an iron rich environment, suggesting the existence of an alternative pathway for iron transport into cells.

In order to understand the mutations or polymorphisms in the overall copper transport function of ATP7B, we were using complementation of the

high-affinity iron-uptake deficiency phenotype of the ccc2 mutant as an indirect assay and confocal microscopy for ATP7B localization. The assay is based on the complementation of null mutant, △ccc2 yeast by mutant ATP7B to determine the effect of missense or nonsense mutations on ATP7B function in WND. When yeast lack Ccc2p, the yeast become lack high-affinity iron uptake through Fet3p, permitting them unable to grow on iron-limiting conditions. ATP7B variant proteins retaining all or most copper transport activity may be rare normal variants that have not yet found previously or variant proteins with normal copper transport activity that are mislocalized in hepatocytes. This study describes the copper-dependent localization or mislocalization of variant ATP7B proteins by confocal microscopy and yeast assayed for ATP7B function. We are aimed to understand the interrelation between ATP7B intracellular copper-dependent localization and copper transport function.

II. MATERIALS AND METHODS

Construction of mutated *ATP7B* cDNAs

The 4.7 kb full length cDNA of *ATP7B* cloned into pBlueScript II KS(-) was kindly donated and also the yeast expression vector, pSY114 and *Saccaromyces cerevisiae* YPH499(△*ccc2)* were willingly contributed from Dr. Terada and Dr. Sugiyama (Akita University School of Medicine, Japan). To obtain point-mutated cDNAs utilized in this study, PCR-based site-directed mutagenesis was performed. First, primers were designed to amplify a *Bgl* II-*Eco*R I fragment (cDNA nucleotide; nt 163-1488) from *ATP7B* cDNAs with or without a Kozak sequence (CCATT) just before the start codon (Table II-1). Subsequently, the digested PCR products (*Bgl* II-*EcoR* I) were directly inserted into the mammalian expression vector, pEGFPC1 (BD Biosciences, Palo Alto, USA). A second *EcoR* I-*BamH* I fragment (nt 1488-4557) amplified from the cDNAs was also ligated into the same expression vector and used as template for mutagenesis PCR. The complete 4.4 kb cDNA of pEGFPC1-ATP7B which contains the entire coding region of the wild type of ATP7B was generated. The presence of mutation and the fidelity of the entire cDNA sequence were confirmed using a 3100 ABI Sequence analyzer (ABI system, Foster, USA).

Yeast strains, growth conditions and transfomations

The *CCC2* gene was disrupted from chromosomal DNA of *Saccharomyces cerevisiae* YPH499 (*MAT*a, *ura3-52, leu2-△1, trp1-△63,his3-△200, ade2-101,lys2-801*) △ccc2 yeast cells were transformed with the constructed cDNA by the modified lithium acetate method and the transformants were selected on solid synthetic dextrose (SD) medium (0.67% yeast nitrogen base without amino acids, 2% glucose, 2% agar) supplemented with adenine, uracil, tryptophan, and lysine. For the metal dependent complementary assay, histidine (20 ㎎/㎖) was added to the same medium with 2% agarose instead of 0.7% agar. The selected transformants were grown at 30℃ for 4 days on the test medium containing 400 uM of bathocuproine dissulfonate and/or 400 uM ferrozine [3-(2-pyridyl)-5.6-bis(4-phenylsulfonic acid)-1,2,4-triazine], or without both chelators.

Table II-1. PCR primers used for cloning of wild type *ATP7B* cDNA coding sequence

Bgl II-GFPC1F	GGA ***AGATCT*** CCACC [a)] ATG CCT GAG CAG GAG AGA CAG
EcoR I-GFPC1R	CTG CAC AGA TGT AGG TGT ACC
EcoR I-GFPC1F	CTG AAA GCT GTT CTA CTA ACC
BamH I-GFPC1R	CG ***GGATCC*** GAT GTA CTG CTC CTC ATC CC

[a)] Kozak sequences underlined were inserted just before start condon. Italic bold nucleotides were used as a restriction enzyme site for plasmid manipulation.

Transient transfection

The 4.4 kb full-length cDNA of *ATP7B* and those variants of site-directed mutation were constructed as described above. For transient transfection into mammalian cells, expression plasmids were isolated from 100 ml of bacteria cultures grown in Lubria-Barteny (LB) broth medium containing 50 ㎍/㎖ kanamycin using ion exchange chromatography (Promega, Madison, USA) according to the manufacturer's protocol.

Prior to transfection, cells were plated to 70-80% confluence (4 X 10^5 cells/35-mm well) onto sterile glass coverslips in six-well tissue culture plates, in 2 ml of medium. The cells grown overnight (18-20 hours) were transfected with the mixture of 2.0 ㎍ of plasmid DNA containing 12.4 ㎕ of 2 M calcium solution and 100 ㎕ 2X HEPES-buffered saline (HBS) (BD Biosciences Clontech, CalPhos™ , USA) according to the manufacturer's protocols. The plasmid DNA of 2 μg with an empty vector, pEGFPC1 were transfected as a control. The cells were incubated with the transfection mixture for 3-4 hours, 37℃, followed by replacement with 10% MEM medium. Following overnight growth (24-30 hours), the medium was left unsupplemented, or was supplemented with 100 uM copper chelator, BCS. The cells were further incubated for 2-3 hours prior to immunofluorescence experiments.

Confocal images with indirect immunofluorescence

Cells attached to coverslips were transferred to a new six-well plate and processed for immunofluorescence staining. The cells were rinsed twice with 1 X PBS then fixed for 15 minutes at room temperature with 4% paraformaldehyde (pH 7.2) in PBS. The fixed cells were rinsed twice with PBS then permeabilized by incubation for 10 minutes in 0.2% Triton X-100 in PBS. The permeablilzed cells were blocked with 1% bovine serum albumin (BSA) in PBS for 1 hour. To detect the Golgi network, Golgi-58K antibody (Abcam, Cambridge, UK) was diluted at a 1:1000 ratio. The primary antibody was incubated for 90 minutes at room temperature. The cells were rinsed twice with PBS. Secondary antibody incubation was done at room temperature for 1 hour in 1% blocking buffer using a 1:200 dilution of goat anti-mouse IgG (H+L) (Alexa Fluor® 555 Molecular Probes, Eugene, USA). Then washed 3 times for 10 minutes each with PBS. Coverslips were then mounted onto slides using mounting media (DakoCytomation, Carpinteria, USA) and stored in the slide box until reading. Confocal microscopy was performed on a fluorescence microscope using a 100 X objective lens and oil immersion. Photographs were saved in a file with the assistance of instrumental lab-technician.

Cell culture

COS-7 cells were purchased from American Type Culture Collection (ATCC, Manassas, USA). COS-7 cells were stably maintained in Dulbecco's modified Eagle's medium (Gibco BRL, Gaithersburg, USA) containing 10% heat-inactivated fetal bovine serum, penicillin (100 U/ml) and streptomycin (100 μg/ml) (Gibco BRL, Gaithersburg, USA). The cells were maintained under 5% CO_2 incubation at 37℃.

Plasmid preparations

The cDNAs of *ATP7B* gene were established in mammalian expression plasmid vector and/or yeast expression plasmid vector, designated as pEGFPC1-ATP7B and pSY114-ATP7B, respectively.

The plasmid DNAs used in all experiments were prepared with DNA purification columns (Quiagen, Valencia, USA) according to manufacturer's instructions. Following isopropanol precipitation, the plasmid was dissolved in TE buffer (10 mM Tis·Cl, 1 mM EDTA, pH 8.0), and the plasmid was precipitated with 2.5 volumes of ethanol. After washing the pellet in 70% ethanol, the plasmid was dissolved in TE buffer to obtain a final concentration of 0.5-1.0 ㎎/㎖.

Transformation of recombinant plasmids

Transformation of all plasmids was carried out with the chemical methods (Hanahan *et al.*, 1983 and Okayama *et al.*, 1987). The competent cells, JM109 were grown in LB medium (tryptone 1%; yeast extract 0.5%; NaCl 1%). The JM109 was *Escherichia coli* K12 strain and its genotype has been described as *recA*1, *endA*1, *gyrA*96, *thi*, *hsdR*17 (r_k^-,m_k^+), *supE*44, *relA*1, Δ(*lac-proA,B*), F' *traD*36, *proA,B* and *lacIqZ*-M15. To prepare an ultra-competent cell, transformation buffer was made from the components (10 mM Pipes, 55 mM $MnCl_2$, 15 mM $CaCl_2$, 250 mM KCl) and the pH was adjusted to 6.7 with KOH. The solution was sterilized by filtration through a prerinsed 0.45 ㎛ filter and stored at 4℃. A frozen stock (in LB containing 20% glycerol) of JM109 was thawed, streaked on an LB agar plate, and cultured for overnight at 37℃. A colony was isolated with a sterile inoculation loop, inoculated to 100 ml of SOB medium in a 500 ㎖ flask, and grown to an OD_{600} of 0.6 at 18℃, with vigorous shaking (200 rpm). The flask was removed from the incubator and placed on ice for 10 minutes. The culture was transferred to 50 ml centrifuge bottles and spun at 3,000 g for 10 minutes at 4℃. The pellets were gently resuspended in 1/3 volume of ice-cold TB of total volume, incubated in an ice bath for 10 minutes, and spun down as described above. The cell pellet was gently resuspended in 1/12 volume of ice-cold TB, and DMSO (dimethyl sulfoxide) was added with

gentle swirling to a final concentration of 7%. After incubating in an ice bath for 10 min, the cell suspension was dispensed by 1 ml into cell freezing tubes, and immediately stored by soaking in liquid nitrogen tank and stored in a deep freezer (-80℃). A tube of competent cells was thawed in water bath at 37℃. One microliter of recombinant plasmid was added to the competent cell, and the cells were incubated in an ice bath for 30 minutes. Then the cells were heat-pulsed without agitation at 37℃ for 30 seconds twice and transferred to an ice bath for 2 minutes. After 0.9 ml of LB was added, the tubes were placed in a 37 ℃ incubator and shaken vigorously for 1 hour before spreading on LB agar plate, containing ampicillin (50 ㎍/㎖) or kanamycin (50 ㎍/㎖). Colonies were collected after overnight incubation (12-20 hours) at 37 ℃.

Site-directed mutagenesis for construction of mutant *ATP7B*

The site-directed mutagenesis was performed with a PCR-based *Dpn* I-treatment method (Li S *et al.*, 1997). The PCR reaction was carried out in 20 ㎕ reaction mixture with 1 unit of *LA* DNA *Taq* polymerase (TAKARA, Shiga, Japan), containing 50 ng of template plasmid DNA consisting of the *ATP7B* cDNA cloned in pSY114 and pEGFPC1, 10 pmole of specific primers, 200 uM of each dNTPs and *LA* reaction buffer (200 mM Tric-Cl, 100 mM KCl, 1 mM DTT, 100 mM $(NH_4)_2SO_4$, 20 mM $MgSO_4$, 1% Triton X-100, 1 ㎎/㎖ acetylated BSA, pH 8.8). After PCR reaction was completed, 5 ㎕ of the PCR product was run on a 1% agarose gel to confirm the expected amplified products. The PCR products were resuspended in 10 ㎕ of ligase buffer with 1 unit of T4 DNA ligase (Promega, Madison, USA) and incubated at 14℃ for 3-16 hours. Then the ligation mixture solution was placed in a water bath with 10 units of *Dpn*I (Promega, Madison, USA) at 37℃ for 90 minutes. Then, the reaction mixture was incubated again at 65℃ for 10 minutes to heat-inactivate the T4 DNA ligase. One microliter of mixture was transformed to JM109 competent cells following a modified Inoue method (Inoue *et al.*, 1990) as described above. The mutation sites were confirmed by sequence analysis with BigDye termination version 3.0 (ABI, Foster, CA, USA). The sequences of oligonucleotides for site-directed mutagenesis are listed in Tabel II-2.

III. RESULTS

Construction of the expression vector of wild type *ATP7B*

The cDNA PCR primers were designed to amplify desired regions from pBluscript SK(-) cloned-ATP7B (Table II-1). PCR reaction was performed in a thermal cycler. Two PCR products were ligated at the restriction enzyme sites, *Bgl* II-*Eco*R I, *Eco*R I-*Bam*H I to generate an in-frame fusion clones. The expression plasmid, encoding the entire coding region of the wild type of *ATP7B*, pEGFPC1-ATP7B was generated as described above. There were no missense or nonsense point mutations in full sequences.

Mutated *ATP7B* introduced into a mammalian expression vector

The expression plasmids, pEGFPC1-ATP7B and pEGFPC1-MUT (p.C656X, p.G891D, p.T1029I, p.T1031A, p.V1106I), containing the entire coding region of the mutant form of *ATP7B* gene were constructed by PCR-based site-directed mutagenesis (Table II-2). Mutant sequences were confirmed by sequence analysis.

Table II-2. Sequences of oligonucleotides used in the site-directed mutagenesis of wild type cDNA of the *ATP7B* gene

Mutations	Sequence	
	Sense	Antisense
p.C656X	5-CTT TCC TGT G**A**A GCC TGG TG-3	5-CAC CAG GCT **T**CA CAG GAA AG -3
p.G891D	5-ACC CAC GTG G**A**C AAT GAC AC-3	5-GTG TCA TTG **T**CC ACG TGG GT-3
p.T1029I	5-GAC AAG A**T**T GGC ACC ATT ACC-3	5-GGT AAT GGT GCC A**A**T CTT GTC-3
p.T1031A	5-GAC AAG ACT GGC **G**CC ATT ACC-3	5-GGT AAT GG**C** GCC AGT CTT GTC-3
p.T1106I	5-GGT GCA AA**A** TCA GCA ACG TGG-3	5-CCA CGT TGC TGA **T**TT TGC ACC-3
p.R778L	5-GCC **T**GT GGC TGG AAC ACT TGG-3	5-CCA AGT GTT CCA GCC AC**A** GGC
p.S406A	5-ATA ATC CC**G** CTG TAA TTA GC-3	5-GCT AAT TAC AG**C** GGG ATT AT-3
p.K832R	5-GAT ATC GTC A**G**G GTG GTC CCT G-3	5-CAG GGA CCA CC**C** TGA CGA TAT C-3
p.K952R	5-GTT GTT CAG A**G**A TAC TTT CC-3	5-GGA AAG TAT **C**TC TGA ACA AC-3

Generation of mutant yeast constructs to analyze the restoration of △ccc2

To determine the functional significance of an amino acid change identified from hospitalized patients, a series of mutant constructs into yeast vector pSY114-MUT (p.C656X, p.G891D, p.T1029I, p.T1031A, p.V1106I, pS406L, pK832R, pK952R, p.R778L) were generated in the full-length mutant cDNA by PCR based site-directed mutagenesis. Mutant sequences were confirmed by sequence analysis.

Comparative alignment analysis of the ATP7B

To obtain information regarding the complete amino acids of *ATP7B* with its orthologues, sequence alignments were performed in comparison with its paralogous copper-transporting protein, ATP7A and with its orthologues; mouse, rat, sheep, and yeast. Comparative alignment analysis revealed that the novel mutations were high conservation of peptide sequence. The alignment analysis showed that the DKTGT motif was the most conserved even in a yeast strain (*Saccaromyces seravisiea*) (Fig. II-9). The relatively high conservation of this motif among different species suggests its functional importance.

Assessment of copper transport function by the yeast growth assay

To identify whether the ATP7B variants have an effects on ATP7B copper transport function, mutant yeast constructs were transformed into △ccc2 yeast. The transformed strains were assayed for their ability to complement the mutants with low-affinity iron-uptake (Fig. II-1). Growth rates of the mutant transformed yeast were measured in an iron-limited medium and compared between ccc2 mutants and ATP7B-transformed construct (Fig. II-5). A p.C656X-expressing mutant yeast lacking the entire of C-terminus was completely unable to grow in the iron-limited medium (Fig. II-2,3). No growth of p.T1929I, p.T1031A mutant yeast were also observed in the iron-limited medium (Fig. II-4). In contrast, a pG891D mutant yeast inactivated some growth under these conditions, suggesting in partial restoration of ATP7B function (Fig.II-2,3). This consequence also correlates with genotype-phenotype. On the other hand, a p.R778L mutant yeast such as disease-causing mutations disturbed the ATP7B transporting activity (Fig. II-2,3). Thus, this yeast was unable to grow in the medium, accordant with the phenotype with WND patient. Postive control groups, containing single nucleotide polymorphic change, p.406L, p.K832R and p.K952R, exhibited compatible growth appearance with the ATP7B rescued yeast (Fig. II-2).

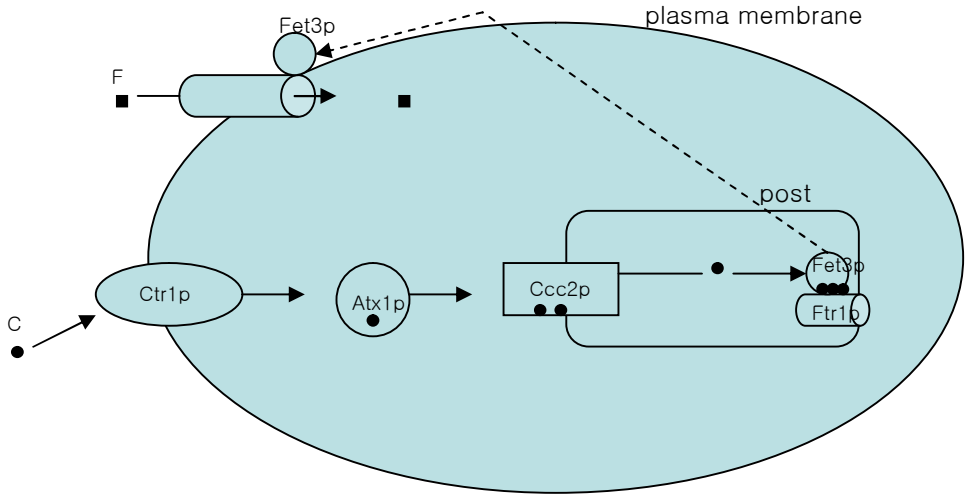

Figure II-1. A model of copper and iron homeostasis in yeast.

The plasma membrane protein, Ctr1p transports coppers into the cytoplasm (Dancis *et al*. 1994). Coppers are carried in the cytoplasm by the copper chaperone, Atx1p (Lin *et al*. 1997), which delivers coppers to Ccc2p. Coppers are supplied by Ccc2p, within a post-Golgi compartment (Yuan *et al*. 1997), to the plasma membrane oxidase Fet3p, which functions with the high-affinity iron transporter Ftr1p to import iron (Stearman *et al*. 1996). When yeast cells lack Ccc2p, coppers are not incorporated into Fet3p, and subsequently the cells lack iron uptake efficiently (Yuan *et al*. 1995). In the absence of high-affinity iron uptake, ccc2 mutant yeast cells were unable to grow on the iron-limited medium. This diagram was adapted from recent report (Forbes JR *et al*., 1998).

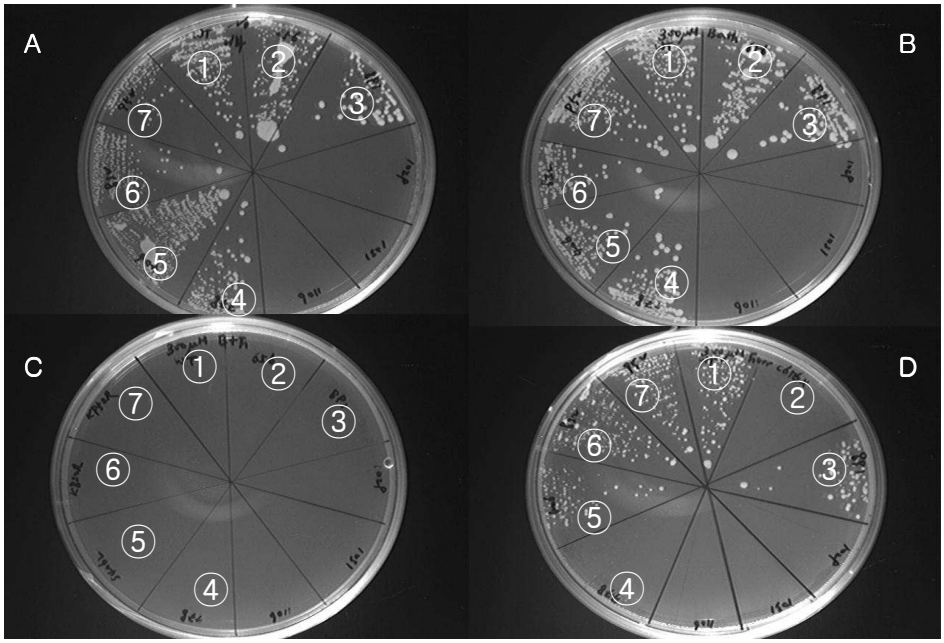

Figure II-2. Metal dependent yeast complementation assay (p.C656X, p.G891D, p.R778L, p.S406L, p.K832R, p.K952R).

Metal dependent yeast complementation assay for the growth of the yeast Δccc2 strain transformed with full-length *ATP7B* cDNA and its mutant *ATP7B*. The Δccc2 yeast cells were transformed with the mutated *ATP7B* cDNAs. A, no chelators; B, 300 uM bathocuproine disulfonate for chelating copper; C, 300 uM bathocuproine disulfonate and 300 uM ferrozine; D, 300 uM ferrozine for chelating iron. Strains grown on each plate Δccc2 transformed with wild type *ATP7B* (area ①), Δccc2 with p.C656X (area ②), Δccc2 with p.G891D (area ③), Δccc2 with p.R778L (area ④), Δccc2 with p.S406L (area ⑤), Δccc2 with p.K832R (area ⑥), and Δccc2 with p.K952R (area ⑦).

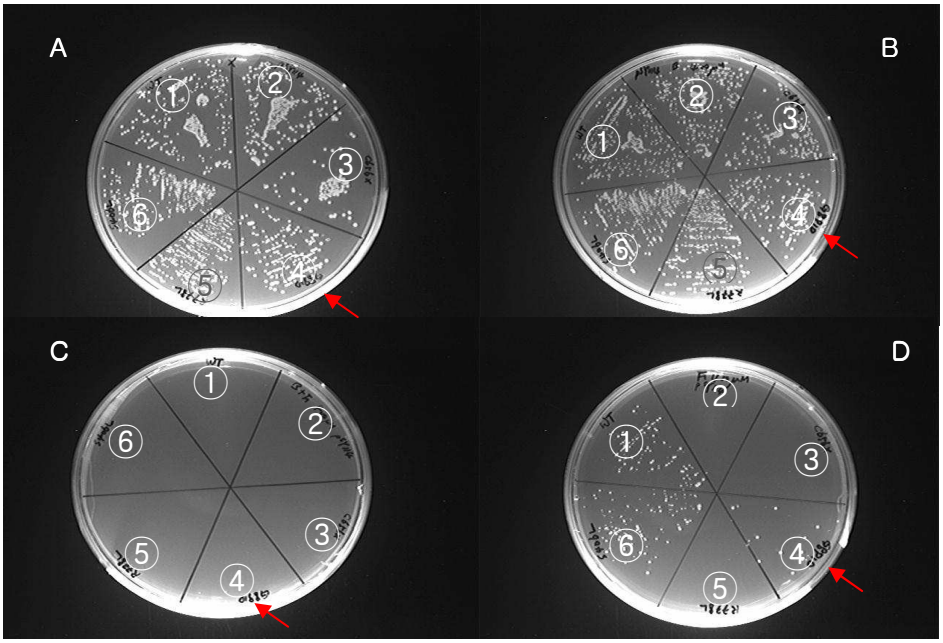

Figure II-3. Metal dependent yeast complementation assay (p.C656X, p.G891D, p.R778L, p.S406L).

Metal dependent yeast complementation assay for the growth of the yeast Δccc2 strain transformed with full-length *ATP7B* cDNA and its mutated *ATP7B*. An arrow indicates that restoration of p.G891D proteins were proven to colonize partially depending on the iron concentration. A, no chelators; B, 400 uM bathocuproine disulfonate for chelating copper; C, 400 uM bathocuproine disulfonate and 400 uM ferrozine; D, 400 uM ferrozine for chelating iron. Strains grown on each plate Δccc2 transformed with wild type *ATP7B* (area ①), Δccc2 with vector alone (area ②), Δccc2 with p.C656X (area ③), Δccc2 with p.G891D (area ④), Δccc2 with p.R778L (area ⑤), and Δccc2 with p.S406L (area ⑥).

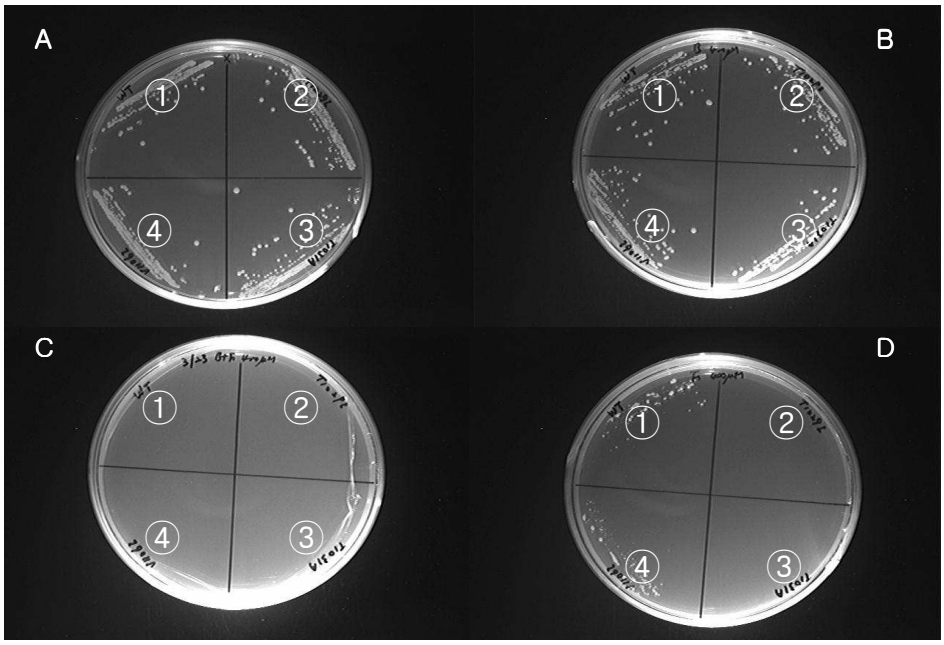

Figure II-4. Metal dependent yeast complementation assay (p.T1029I, p.T1031A, p.V1106I).

Metal dependent yeast complementation assay for the growth of the yeast Δccc2 strain transformed with full-length *ATP7B* cDNA and its mutated *ATP7B*. The Δccc2 yeast cells were transformed with the mutated *ATP7B* cDNAs and the transformants were selected on solid synthetic dextrose (SD) medium as described in materials and methods. A, no chelators; B, 400 uM bathocuproine disulfonate for chelating copper; C, 400 uM bathocuproine disulfonate and 400 uM ferrozine; D, 400 uM ferrozine for chelating iron. Strains grown on each plate Δccc2 transformed with wild type *ATP7B* (area ①), Δccc2 with p.T1029I (area ②), Δccc2 with p.T1031A (area ③), and Δccc2 with p.V1106I (area ④).

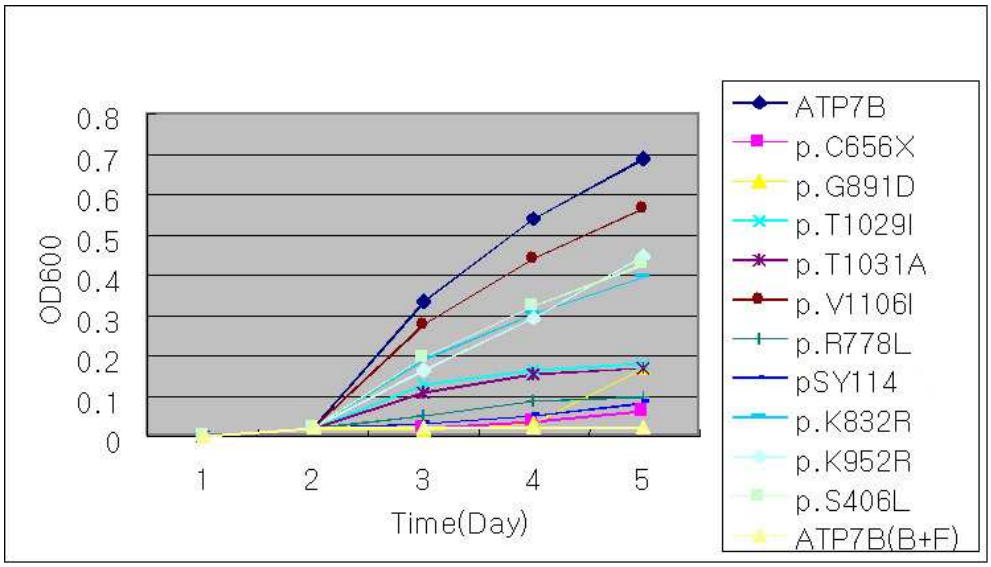

Figure II-5. Quantitation of restored Δccc2 transformed with wild type *ATP7B* and △ccc2 with its mutant yeast.

Growth curves were generated in the iron-limited medium (ferrozine 400 uM) of yeasts expressing normal or mutant ATP7B over a 5-day period at 30℃. ATP7B; Δccc2 transformed with *ATP7B* cDNA, p.C656X; Δccc2 with pSY114-p.C665X, p.G891D; Δccc2 with pSY114-p.G891D, p.T1029I; Δccc2 with pSY114-p.T1029I, p.T1031A; Δccc2 with pSY114-p.T1031A, p.V1106I; Δccc2 with pSY114-p.V1106I, p.R778L; Δccc2 with pSY114-p.R778L, pSY114; Δccc2 with vector alone, p.K832R; Δccc2 with pSY114-p.K832R, p.K952R; Δccc2 with pSY114-p.K952R, p.S406L; Δccc2 with pSY114-p.S406L and ATP7B (B+F) containing metal ion chelators (400 uM bathocuproine disulphonate and ferrozine); Δccc2 with *ATP7B* cDNA.

Localization of human ATP7B mutant proteins

The novel mutant protein constructs, pEGFPC1-p.C656X, p.G891D, p.T1029I, p.T1031A, and p.V1106, were expressed in COS-7 cells, each of which showed abnormal or partially normal targeting in *trans*-Golgi network other than p.V1106I, depending on copper condition. suggesting that the copper transporting activity was working normally *in vitro* system. A confocal images of pEGFPC1-p.C656X were visualized as a representative of deletion of C-terminus, which demonstrated a severely defective ATP7B function in the previous yeast complementation assay. The majority of mutant p.C656X protein was distributed throughout the transfected cells, indicating the mis-localization of ATP7B protein, which was accordance with consequences in the yeast system (Fig. II-7). A pEGFPC1-p.G891D mutant ATP7B was partially localized to the position of the *trans*-Golgi network when transfected into COS-7 cells. This phenomenon was virtually observed in all expressed cells (Fig. II-8). A pEGFPC1-p.T1029I, p.T1031A, mutant ATP7B proteins were predominantly localized to the perinuclear region of the *trans*-Golgi network or even to the nuclear compartment (Fig. II-7,8). Although a pEGFPC1-p.V1106I was inefficiently transfeced in COS-7 cells, the patterns of immunofluorescent images using a confocal microscope were compatible with the Golgi -58K marker. It revealed that the pEGFPC1-V1106I protein colocalized with wild type ATP7B in COS-7 cells (Fig. II-6).

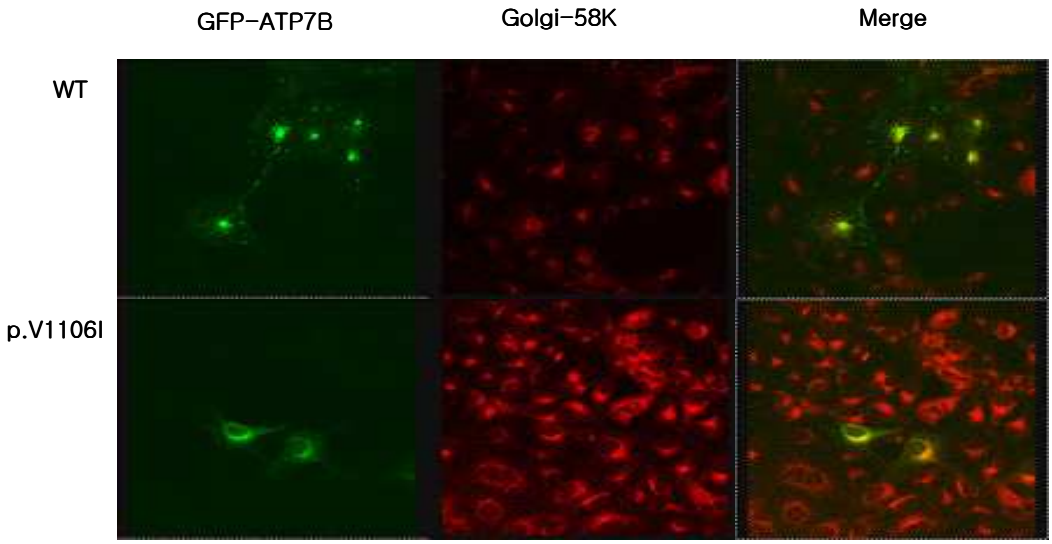

Figure II-6. Confocal laser microscopic images of GFP-ATP7B transfected COS-7 cells incubated for 30 hours with a Golgi marker, Golgi-58K (WT & p.V1106I).

COS-7 cells were transiently transfected with an ATP7B expression construct, pEGFPC1-ATP7B or a variant ATP7B expression construct, pEGFPC1-p.V1106I. The pEGFPC1-ATP7B or p.V1106I proteins in *trans*-Golgi compartment were visualized by immunostaining. The primary antibody was incubated with the mouse monoclonal Golgi-58K antibody which was detected by the labeled goat anti-mouse IgG (H+L) (Alexa Fluor® 555).

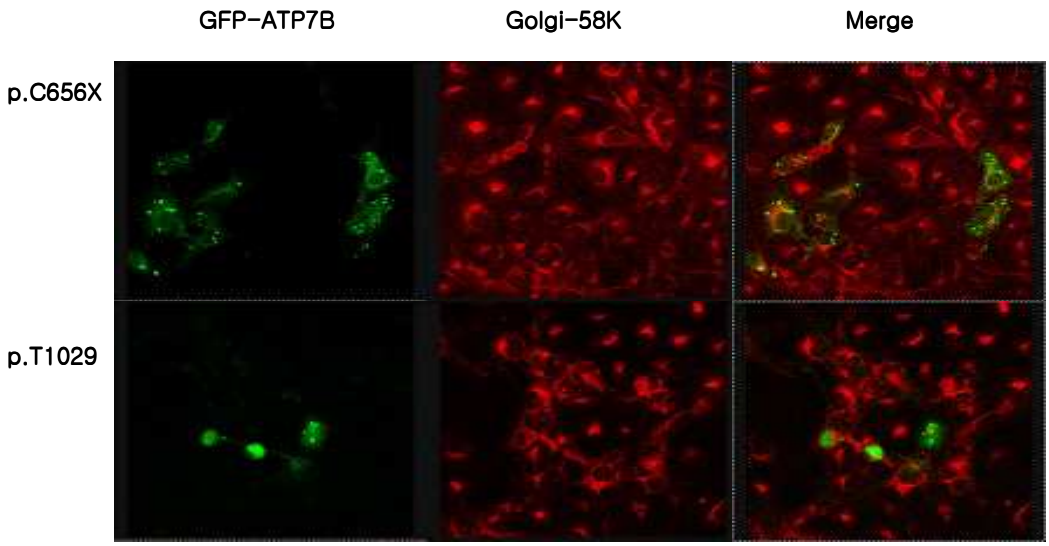

Figure II-7. Confocal laser microscopic images of GFP-ATP7B transfected COS-7 cells incubated for 30 hours with a Golgi marker, Golgi-58K (p.C656X & p.T1029I).

COS-7 cells were transiently transfected with an variant ATP7B expression construct, pEGFPC1-p.C656X or a variant ATP7B expression construct, pEGFPC1-p.T1029I. The scattered ATP7B of mutant pEGFPC1-p.C656X was visualized to be dotted with green fluorescence within the whole cytoplasm (Top). The aberration of mutant pEGFPC1-p.T1029I protein was observed in the nucleus (Bottom). The primary antibody was incubated with the mouse monoclonal Golgi-58K antibody which was detected by the labeled goat anti-mouse IgG (H+ L) (Alexa Fluor® 555).

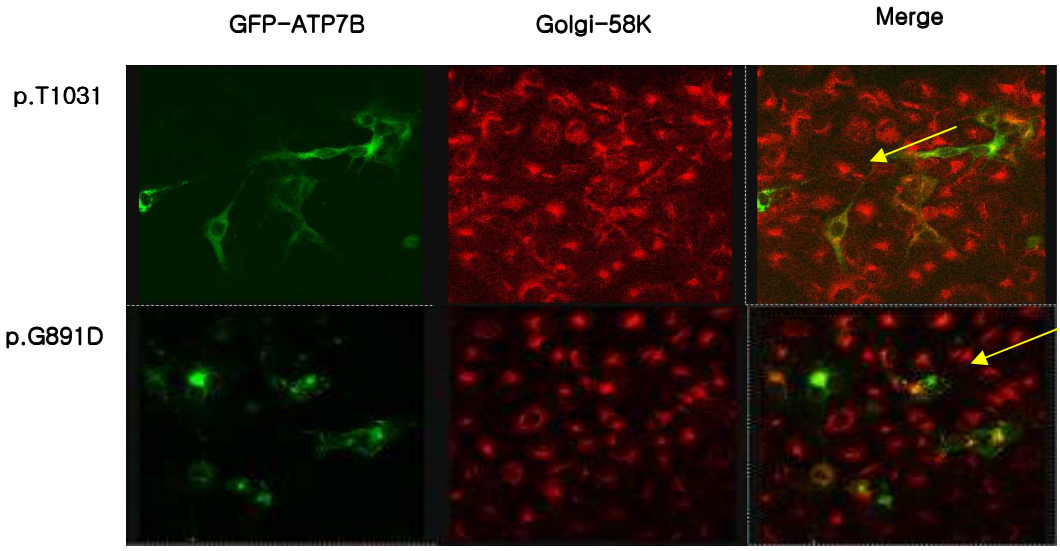

Figure II-8. Confocal laser microscopic images of GFP-ATP7B transfected COS-7 cells incubated for 30 hours with a Golgi marker,Golgi-58K (p.G891D & p.T1031A).

COS-7 cells were transiently transfected with an variant ATP7B expression construct, pEGFPC1-p.T1031A and pEGFPC1-p.G891D. The mutant ATP7B of pEGFPC1-p.G891D was partially colocalized in *trans*-Golgi compartment by immunostaining The mutant ATP7B of pEGFPC1-p.T1031A was mislocalized in the perinuclear regions. An arrow indicates the mislocalization of the mutant ATP7B. The primary antibody was incubated with the mouse monoclonal Golgi-58K antibody which was detected by the labeled goat anti-mouse IgG (H+L) (Alexa Fluor® 555).

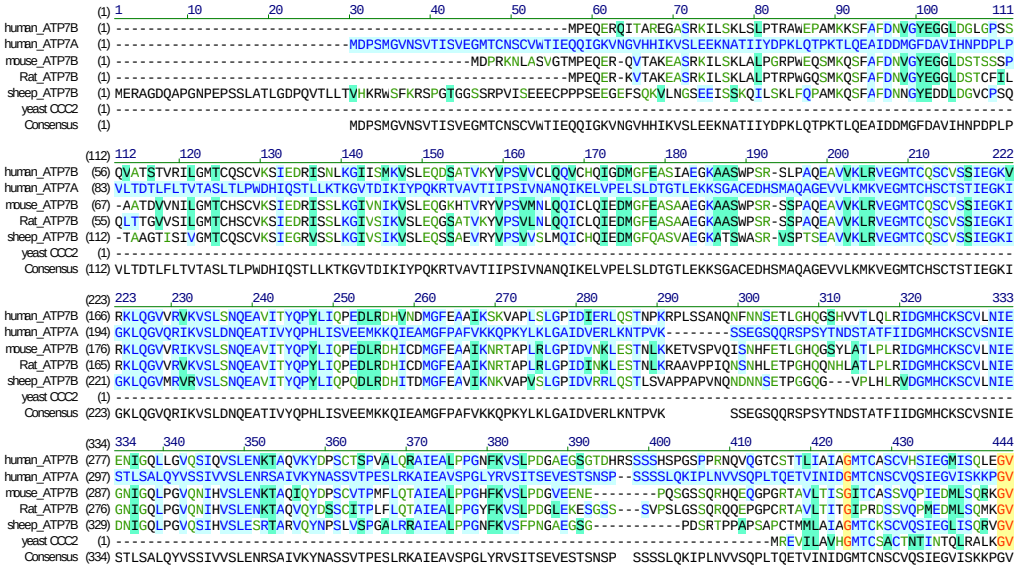

p.E412X

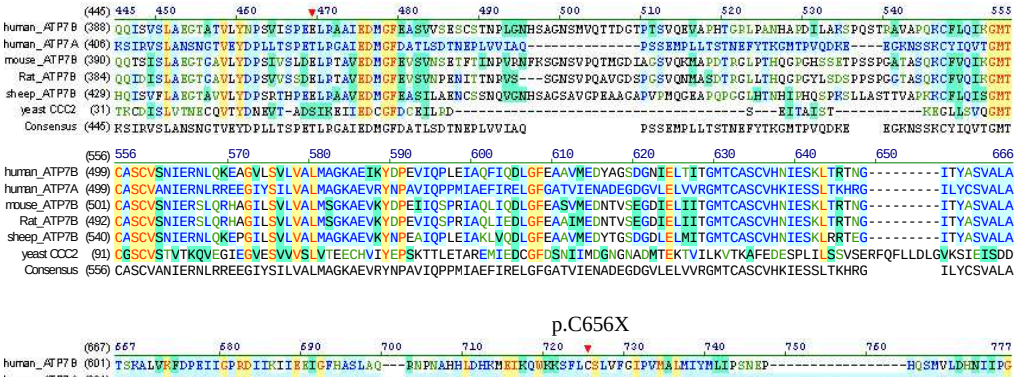

p.C656X

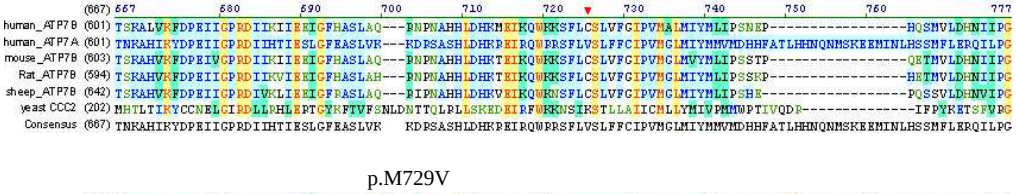

p.M729V

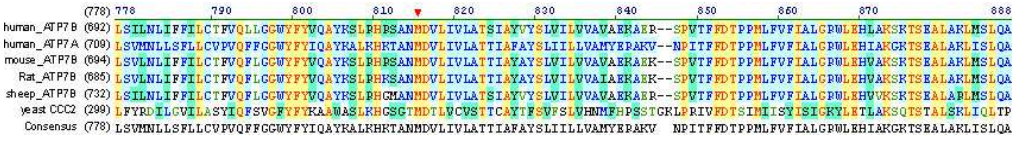

p.G891D

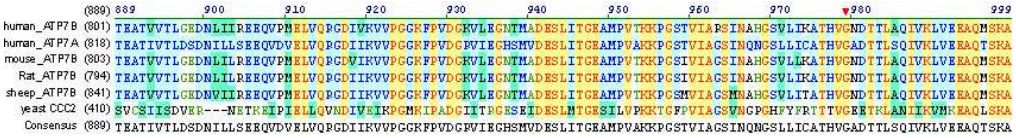

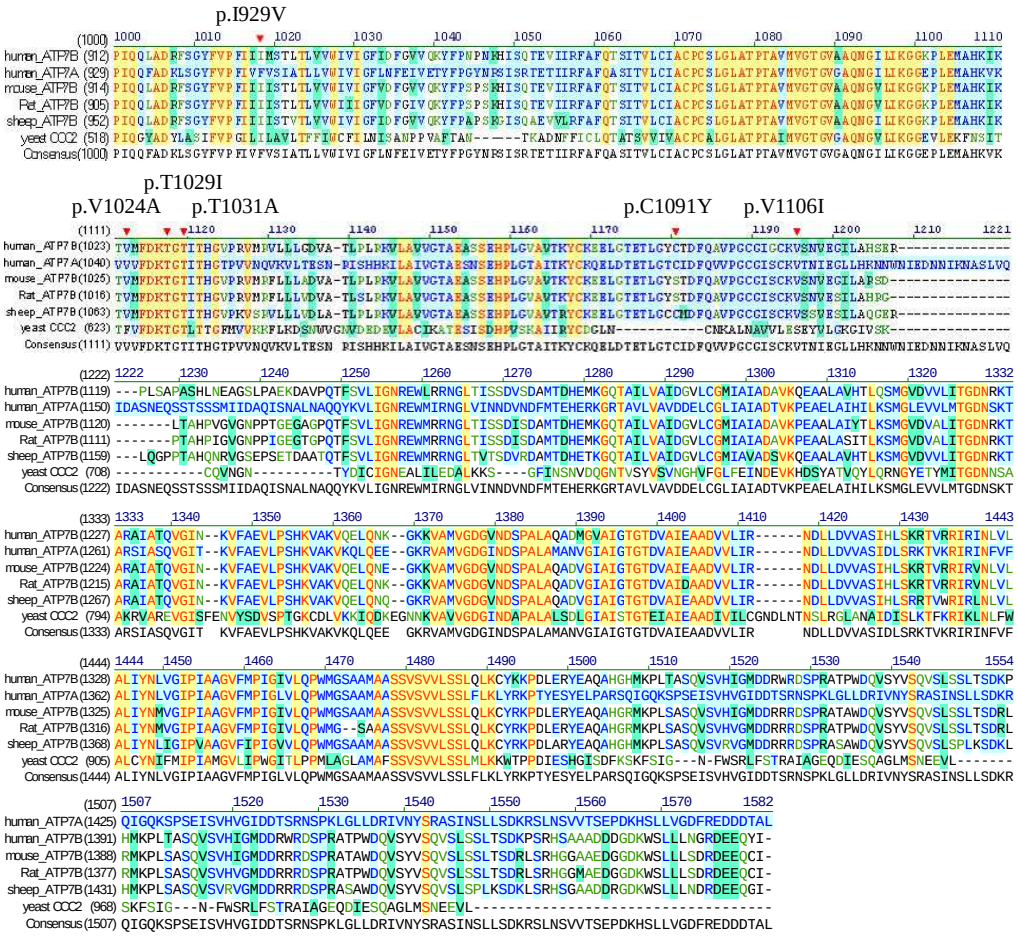

Figure II-9. Comparative alignment analysis of human ATP7B protein and other orthologous amino acids of ATP7B proteins.

Comparative alignment analysis showed evolutionarily conserved sequences in the areas of novel missense/nonsense mutations. Comparative alignment analysis of peptide sequences of 6 strains was carried out with VectorNTI™ BROSUM protocol of Infomax (Invitrogen, Carlsbad, USA). The 5 strains were *Homo sapiens* (human), *Mus musclus* (mouse), *Rattus novegicus* (rat), *Ovis aries* (sheep), and *Saccharomyces cerevisiae* (yeast).

IV. DISCUSSION

The yeast *Ccc2* gene, encoding a copper transporting P-type ATPase, is an orthologue of the human ATP7B. The yeast △ccc2 mutant lacking the *Ccc2* gene was unable to colonize on the iron-limiting media due to reduced iron uptake resulting from the disturbed incorporation of copper into Fet3p (Fig. II-1). Recent reports suggested that Ccc2p function was rescued by introducing *cua-1*, encoding a copper transporter of *Caenorhabditis elegans*, into the △ccc2 mutant (Sambongi *et al.*, 1998). The human ATP7B was able to restore the yeast △ccc2 mutant, but mutant pSY114-p.R778L protein, the most common mutation reported in WND in Korean and Asian populations (Yoo HW, 2002; Chuang LM *et al.*, 1996), was unable to recover the yeast △ccc2 mutant on iron-limiting conditions in the yeast complementation system. Characteristics of colony formations showed that yeast pSY114-MUT proteins were not grown on iron-limiting conditions, but pSY114-ATP7B was rescued from the yeast △ccc2 mutant, suggesting the possibility of their novel mutations. The null mutant, demolishing activity of yeast Ccc2p, could be rescued by expression of exogenous human ATP7B protein, suggesting that the ATP7B functions could be evaluated indirectly depending on iron concentrations. The △ccc2 yeast mutants can survive on Synthetic Dextrose (SD) media with copper and/or iron chelator, however the yeasts cannot survive on complete iron depletion media, depending on an iron-

limiting concentration. This result provides an information for indirect testing of the copper transport function via iron uptake (Fig. II-1).

In order to examine the usefulness of yeast complementation assay for the screening of mutant ATP7B function, the pSY114-MUT clones were obtained from the site-directed mutagenesis targeted on full-length cDNA of pSY114-ATP7B. The △ccc2 yeast strains were transformed with the pSY114-p.C656X, p.G891D, p.T1029I, p.T1031A, p.R778L, p.V1106I novel mutants and p.S406A, p.K832R, p.K952R normal variations as positive control. The most frequent mutation in Korean WND patients, p.R778L, represented about 38% of frequency (Yoo HW, 2002). This mutation is located in the 4th transmembrane domain, which may conformational change due to hydrocarbon length and hydrophobicity of leucine from arginine with highly hydrophilicity of relatively long side chains. The partial complementation of Ccc2p function by mutant pSY114-p.G891D might explain the variable clinical manifestations in patients with this mutation. This mutant was virtually colonized in part and demonstrated very low growth rates during a limited period, which corresponded to clinical phenotype. In contrast, the pSY114-p.T1029I, p.T1031A, positioned in the conserved DKTGT motif, which played a critical role in phosphorylation for energy transduction, could not restore the △ccc2 mutant. This finding might correlate with a high incidence of the fulminant hepatitis, even neurological

symptoms, and very low level ceruloplasmin level (<2 ㎎/dℓ). The mutant pSY114-p.V1106I located in the ATP loop domain was completely rescued in this copper-iron dependent yeast system. To examine the possibilities of polymorphism or novel mutation, the normal population on the novel mutations was performed in 50 healthy individuals. However, a patient with pSY114-p.V1106I mutant was turned out as a polymorphism. A variety of phenotypic manifestations with a disease-causing mutation may imply that identification of genetic deficits in WND patients is essential and important steps for discovering mutant ATP7B deficits.

The ATP7B protein was normally localized to the *trans*-Golgi network in transiently transfected COS-7 cells on copper-limiting conditions. A recent study report, claiming the localization of ATP7B to late endosomes rather than Golgi compartment did not document copper concentration in the culture medium, which can be appreciable in the absence of chelators (Harada M *et al.*, 2000). Although the copper is a main driving force of the redistribution of ATP7B into the cytoplasmic vesicles, which remain to be elucidated, the ATP7B containing vesicles derived from the *trans*-Golgi network were studied with human and rat liver and hepatocytes in recent reports (Schaefer *et al.*, 1999; Petris *et al.*, 1999). When immunofluorescence experiments were directly performed by anti-ATP7B antibodies, COS-7 cells normally express ATP7B so that there can be detected some background due

to the endogenous ATP7B protein. Use of commercial GFP-tagged vector system, pEGFPC1, was applied to this experiment. With uncertainty of ATP7B protein activity due to this foreign protein, the overexpression of pEGFP-ATP7B may deteriorate the ATP7B functional activities or induce mislocalization of ATP7B protein in terms of folding topology. However, throughout the COS-7 cells, no targeting problem of normal pEGFPC1-ATP7B was at least detected in any compartment other than *trans*-Golgi network on copper limiting conditions. Determining of the precise subcelluar localization of proteins may be ambiguous due to overexpression-induced artifact. A recent report indicates that even normal protein of ATP7B may be distributed in the endoplasmic reticulum (John RF *et al.*, 2000), rating of 10~20% of transfected cells. This endoplasmic reticulum-associated mistrafficking of normal ATP7B was observed in the cells that were stained strongly. Therefore, the strong green fluorescience was excluded in the study, which was easily distinguished from the dimmed transfected cell populations for both normal and mutant ATP7B protein. Only confocal image data were represented in successfully transfected remainder cells, which expressed mutant ATP7B, where the localization of transfected proteins was expected to be minimally influenced by overexpression. In order to examine more precise assignment of subcellular localization of normal ATP7B and mutant ATP7B, stable transfection experiments should be required for more

accurate localization by electron microscopy. The mutant proteins could presumably be present in lysosomes or proteasomes pathway for the degradation of misfolded proteins.

The p.C656X protein was a rare mutation reported in Korean patients with WND. The p.C656X was initially classified as a mutation of the early truncated protein decay. In both ccc2 yeast mutant and confocal microscopic image data, the properties of p.C656X demonstrated the same results as no growth on the iron-limiting media and mislocalization of ATP7B within the COS-7 cells. Functional analysis in the yeast system revealed that the mutant was not restore ccc2 yeast mutant completely. The confocal image data also showed that the premature shortened protein was dispersedly observed with degradation within the cytoplasm by immunofluorescence microscopy. It was suggested that the proteins were mislocalized, probably due to extensive protein misfolding or nonsense mediated decay.

The p.G891D is a candidate novel mutation based on the population study of normal chromosome. The p.G891D has not been confirmed as a mutation or a rare variant due to the conservative nature of the amino acid substitution. However, according to the yeast functional data, the p.G891D protein had a gradual increase in its ability to restore ccc2 mutant yeast with a slow growth curve, suggesting reduced copper transport ability and recovered ATP7B function, simultaneously. Interestingly, confocal

microscopic results revealed that some ATP7B proteins of p.G891D exhibited partially localization of perinuclear endoplasmic reticulum of COS-7 cells, others were localized to the Golgi network. Thus, the variant p.G891D appears to be rather a protective modifying gene than disease-causing mutation, consistent with no clinical symptoms in patient.

The mutant p.T1029I and p.T1031A, located in the highly conserved DKTGT motif that is the aspartylphosphate intermediate essential for energy transduction, were classified as a novel mutation. Both p.T1029I and p.T1031A mutant proteins were not found to complement ccc2 mutant yeasts distinguishable from the normal ATP7B. The immunofluorescent data of these mutant proteins showed that p.T1029I proteins were likely in part localized into the nucleus when stimulated by copper chelators and were also unable to transport copper to cytoplasmic vesicles when stimulated by copper. The p.T1031A proteins exhibited localization to perinucleus of COS-7 cells, suggesting that p.T1031A proteins were mislfolded, probably due to retention in the endoplasmic reticulum. Both p.T1029I and p.T1031A mutants should be considered as a disease-causing mutation.

The p.V1106I is a candidate mutation, identified in 3 patients with WND, based on the clinical examinations of two biochemical findings, low ceruloplasmin and increased volume of copper urine, indicative of impaired copper transport function. However, yeast functional and mammalian

localization data showed that the p.V1106I protein showed no slight or significant reduction in its ability to restore ccc2 mutant yeasts and appeared to be likely localized to the *trans*-Golgi network, suggesting normal copper transport function which was consistent with asymptomatic symptoms of disease presentation.

The current pathways of ATP7B-mediated copper excretion involve the copper transport from the *trans*-Golgi network to an intracellular vesicular compartments. Then, the copper fuses with the plasma membrane to be allowed the excessive copper to across the plasma membrane and into the bile canaliculus in hepatocytes (Schaefer *et al.*, 1999). Since the mutants of p.T1029I, p.T1031A were largely mislocalized to nucleus or endoplasmic reticulum throughout the cytoplasmic cells, these defective proteins would not mediate effective copper efflux. Similarly, the mutant p.C656X caused WND in patients carrying this mutation because of an inability to redistribute from the Golgi compartment to cytoplasmic vesicles by stimulation of copper. Thus, the mutant p.C656X appeared to be aggregation as if the stars were twinkling inside the cell, preventing effective biliary copper efflux at all times.

These results suggest the necessity for copper dependent redistribution as a requirement of ATP7B for its role in hepatic copper efflux. Most WND patients are compound heterozygotes that make it difficult to define a precise genotype-phenotype correlation for an individual mutation.

Although functional and localization data can provide a mechanism to explain genotypic variation, the overall phenotype of the disease in patients cannot be easily explained. That may be caused by patients' different ingested amounts and accumulations of hepatic coppers at different rates, which may affect disease severity.

The data of yeast complementation assay showed that ATP7B was able to complement the mutant yeast △ccc2, delivering copper to Fet3p, restoring the ability of null mutant △ccc2 or missense mutant ccc2 yeast to grow on iron-limiting conditions, suggesting a reliable assay for the copper transporter function of ATP7B. The confocal data revealed that ATP7B is normally localized into the *trans*-Golgi network and redistributed into the intracellular vesicular compartment by stimulation of copper, suggesting that the copper transport function is related with the trafficking of ATP7B proteins. In conclusion, the yeast complementation assay and confocal microscopic evaluation are useful tools for a functional study on the mutant ATP7B protein.

CONCLUSIONS

To identify the molecular defects of WND patients in Korea, human *ATP7B* gene was sequenced in 125 unrelated patients. This study aimed to establish the system for the screening of molecular deficits, which could distinguish from novel mutations and rare polymorphisms. In order to do this strategy, first yeast complementation assay was set up on behalf of functional characterization of molecular genetic defects. Second, a confocal laser microscopy was utilized to demonstrate the localization of wild and/or mutant types of ATP7B protein expression in COS-7 cells.

1. Thirty different mutations were identified in 125 patients in 120 unrelated Korean patients with WND. Of the mutations, ten were novel mutations, consisting of 8 missense mutations, and 2 nonsense mutations.

2. In the rate of mutation was 75.6% (189/250) of alleles on direct sequencing of all exons of the *ATP7B* gene in the 125 Korean patients with WND.

3. Four different mutations in exon 8 were found in 41.2% of alleles, three different mutations in exon 11 were found in 9.6% of alleles, and

three different mutations in exon 18 were found in 7.6% of alleles, thereby indicating that exons 8, 11 and 18 were three important exons for detecting mutations in Korean patients with WND. In particular, the p.R778L mutation in exon 8 was found in 39.6% of these Korean patients at least in one allele. Twenty-four patients with WND were homozygotes for p.R778L and 51 patients with WND were heterozygotes for p.R778L.

4. The 4,398 base-pair *ATP7B* gene that encodes a copper-transporting ATPase has been cloned into the mammalian expression vector, pEGFPC1 (4.7kb). The clone, pEGFPC1-ATP7B was confirmed no mutation by direct sequencing.

5. Site-directed mutagenesis was performed on the pEGFPC1-ATP7B clone, producing the same novel mutant types as obtained from the genotypic results; p.C656X, p.G891D, p.T1029I, p.T1031A, and p.V1106I.

6. Nine mutants of ATP7B recombinant yeast vector were constructed by site-directed mutagenesis; p.C656X, p.G891D, p.T1029I, p.T1031A, p.V1106I, p.S406L, p.K832R, p.K952R, and p.R778L.

7. The novel mutations identified in this study were highly reliable except p.V1106I as results of metal-dependent yeast complementation and growth assay; three mutants of p.C656X, p.T1029I and p.T1031A had no growth in the yeast system, suggesting a mutation, three variants of p.S406L, p.K832R and p.K952R were grown on the iron limiting plate. The mutant p.R778L was not grown on the plate on iron-limiting conditions, but the mutant p.G891D was partially rescued in the yeast complementation system. However, the p.V1106I was grown on the media likely as the wild type, suggesting a rare polymorphism.

8. In the localization analysis of the mutant ATP7B with a confocal microscope, the mutant p.C656X was scttered throughout transfected COS-7 cells. The mutant p.G891D was partially localized to the site of the *trans*-Golgi network. Two mutants, p.T1029I and p.T1031A were predominantly mislocalized to nuclear and perinuclear regions, respectively. However, the mutant p.V1106I was normally targeted to the *trans*-Golgi network, which was concordant with the result of the yeast complementation assay.

9. Optimal concentration of copper or iron chelator on the limiting media was evaluated 400 uM in this metal-dependent yeast assay.

10. The yeast complementation assay and confocal microscopic evaluation were useful tools for the functional study on mutant ATP7B proteins.

REFERENCES

Aldridge J, Kunkel L, Bruns G, Tantravahi U, Lalande M, Brewster T, Moreau E, Wilson M, Bromley W, Roderick T. A strategy to reveal high-frequency RFLPs along the human X chromosome. *Am J Hum Genet* **36**: 546-564, 1984.

Askwith, C, Kaplan J. Iron and copper transport in yeast and its relevance to human disease. *Trends Biochem Sci* **23**:135-138, 1998.

Bull PC, Thomas GR, Rommens JM, Fores JR, Cox DW. The Wilson disease gene is a putative copper transporting P-type ATPase similar to the Menkes gene. *Nat Genet* **5**:327-337, 1993.

Chuang LM, Wu HP, Jang MH, Wang TR, Sue WC, Lin BJ, Cox DW, Tai TY. High frequency of two mutations in codon 778 in exon 8 of the *ATP7B* gene in Taiwanese families with Wilson disease. *J Med Genet* **33**:521-523, 1996.

Cullen LM, Prat L, Cox DW. Genetic variation in the promoter and 5'UTR of the copper transporter, *ATP7B*, in patients with Wilson disease. *Clin Genet* **64**:429-432, 20.

Culotta VC, Gitlin JD. Disorders of copper transport. In: Scriver CR, Beaudet

AL, Sly WS, Valle D, eds. The molecular and metabolic basis of inherited disease. New York Volume 3. New York: McGraw-Hill, 3105-3136, 2001.

Dancis A, Yuan DS, Haile D, Askwith C, Eide D, Moehle C, Kaplan J, et al. Molecular characterization of a copper transport protein in *S. cerevisiae*: an unexpected role for copper in iron transport. *Cell* **76**:393-402, 1994.

Duc HH, Hefter H, Stremmel W, Castaneda-Guillot C, Hernandez Hernandez A, Cox DW, Auburger G. His1069Gln and six novel Wilson disease mutations: analysis of relevance for early diagnosis and phenotype. *Eur J Hum Genet* **6**:616-623, 1998.

Emre S, Atillasoy EO, Ozdemir S, Schilsky M, Rathna Varma CV, Thung SN, Sternlieb I, Guy SR, Sheiner PA, Schwartz ME, Miller CM. Orthotopic liver transplantation for Wilson's disease: a single-center experience. *Transplantation* **72**:1232-1236,2001.

Figus A, Angius A, Loudianos G, Bertini C, Dessi V, Loi A, Deiana M, Lovicu M, Olla N, Sole G, et al. Molecular pathology and haplotype analysis of Wilson disease in Mediterranean populations. *Am J Hum Genet* **57**:1318-24, 1995.

Forbes JR, Cox DW. Functional characterization of missense mutations in ATP7B: Wilson disease mutation or normal variant? *Am J Hum Genet* **63**:1663-1674, 1998.

Frommer D, Morris J, Sherlock S, Abrams J, Newman S, Kayser-Fleischer-like rings in patients without liver disease. *Gastroenterology* **72**:1331-1335, 1977.

Gollan JL, Deller DJ. Studies on the nature and excretion of biliary copper in man. *Clin Sci* **44**:9-15, 1973.

Gu YH, Kodama H, Du SL, Gu QJ, Sun HJ, Ushijima H. Mutation spectrum and polymorphisms in *ATP7B* identified on direct sequencing of all exons in Chinese Han and Hui ethnic patients with Wilson's disease. *Clin Genet* **64**:479-484, 2003.

Harada M, Sakisaka S, Terada K, Kimura R, Kawaguchi T, Koga H, Taniguchi E, Sasatomi K, Miura N, Sugiyama T. Role of ATP7B in biliary copper excretion in a human hepatoma cell line and normal rat hepatocytes. *Gastroenterology* **118**:921-928, 2000.

Hellman NE, Gitlin JD. Ceruloplasmin metabolism and function. *Annu Rev Nutr* **22**:439-458, 2002

Inoue H, Nojima H, Okayama H. High efficiency transformation of Escherichia coli with plasmids. *Gene* **30**:23-28,1990.

John RF, Cox DW. Copper-dependent trafficking of Wilson disease mutant *ATP7B* proteins. *Human Molecular Genetics* **9**:1927-1935, 2000.

Kim EK, Yoo OJ, Song KY, Yoo HW, Choi SY, Cho SW, Hahn SH. Identification of three novel mutations and a high frequency of the Arg778Leu mutation in Korean patients with Wilson disease. *Hum Mutat* **11**:275-8, 1998.

Labbe S, Thiele DJ. Pipes and wiring: the regulation of copper uptake and distribution in yeast. *Trends Microbiol* **7**:500-505, 1999.

Li S, Wilkinson MF. Site-directed mutagenesis: a two-step method using PCR and DpnI. *Biotechniques* **23**:588-590, 1997.

Lin SJ, Pufahl RA, Dancis A, O'Halloran TV, Culotta VC: A role for the *Saccharomyces cerevisiae ATX1* gene in copper trafficking and iron transport. *J Biol Chem* **272**:9215-9220, 1997.

Liu XQ, Zhang YF, Liu TT, Hsiao KJ, Zhang JM, Gu XF, Bao KR, Yu LH, Wang MX. Correlation of ATP7B genotype with phenotype in Chinese patients with Wilson disease. *World J Gastroenterol* **15**:590-593, 2004.

Loudianos G, Dessi V, Angius A, Lovicu M, Loi A, Deiana M, Akar N, Vajro P, Figus A, Cao A, Pirastu M. Wilson disease mutations associated with uncommon haplotypes in Mediterranean patients. *Hum Genet* **98**:640-642, 1996.

Loudianos G, Dessi V, Lovicu M, Angius A, Kanavakis E, Tzetis M, Kattamis C, Manolaki N, Vassiliki G, Karpathios T, Cao A, Pirastu M. Haplotype and mutation analysis in Greek patients with Wilson disease. *Eur J Hum Genet* **6**:487-491, 1998.

Loudianos G, Dessi V, Lovicu M, Angius A, Nurchi A, Sturniolo GC, Marcellini M, Zancan L, Bragetti P, Akar N, Yagci R, Vegnente A, Cao A, Pirastu M.

Further delineation of the molecular pathology of Wilson disease in the Mediterranean population. *Hum Mutat* **12**:89-94, 1998.

Loudianos G, Lovicu M, Dessi V, Tzetis M, Kanavakis E, Zancan L, Zelante L, Galvez-Galvez C, Cao A. Abnormal mRNA splicing resulting from consensus sequence splicing mutations of *ATP7B*. *Hum Mutat* **20**:260-266, 2002.

Lutsenko S, Kaplan JH. Organization of P-type ATPases: significance of structural diversity. *Biochemistry* **34**:15607-15613, 1995.

Lutsenko S, Petris MJ. Function and regulation of the mammalian copper-transporting ATPases: insights from biochemical and cell biological approaches. *J Membr Biol* **191**:1-12, 2003.

Moller JV, Juul B, le Maire M. Structural organization, ion transport, and energy transduction of P-type ATPases. *Biochim Biophys Acta* **1286**:1-51, 1996.

Nanji MS, Nguyen VT, Kawasoe JH, Inui K, Endo F, Nakajima T, Anezaki T, Cox DW. Haplotype and mutation analysis in Japanese patients with Wilson disease. *Am J Hum Genet* **60**:1423-1429, 1997.

Okada T, Shiono Y, Hayashi H, Satoh H, Sawada T, Suzuki A, Takeda Y, Yano M, Michitaka K, Onji M, Mabuchi H. Mutational analysis of ATP7B and genotype-phenotype correlation in Japanese with Wilson's disease. *Hum Mutat* **15**:454-462, 2000.

Olivares M, Araya M, Uauy R. Copper homeostasis in infant nutrition: deficit and excess. *J Pediatr Gastroenterol Nutr* **31**:102-111, 2000.

Payne AS, Gitlin JD. Functional expression of the Menkes disease protein reveals common biochemical mechanisms among the copper-transporting P-type ATPases. *J Biol Chem* **273**:3765-3770, 1998.

Petris MJ, Mercer JFB. The Menkes protein (ATP7A; MNK) cycle via the plasma membrane both in basal and elevated extracellular copper using a C-terminal di-leucine endocytic signal. *Hum Mol Genet* **8**:2107-2115, 1999.

Petrukhin K, Lutsenko S, Chernov L, Ross BM, Kaplan JH, Gilliam TC: Characterization of the Wilson disease gene encoding a P-type copper transporting ATPase: Genomic organization, alternative splicing , and structure/function predicting. *Hum Mol Genet* **3**:1647-1656, 1994.

Sambongi Y, Wakabayashi T, Yoshimizu T, Omote H, Oka T, Futai M. *Caenorhabditis elegans* cDNA for a Menkes/Wilson disease gene homologue and its function in a yeast CCC2 gene deletion mutant. *J Biochem* **121**:1169-1175, 1997.

Schaefer M, Gitlin JD. Genetic disorders of membrane transport. IV. Wilson's disease and Menkes disease. *Am J Physiol* **276**:311-314, 1999.

Schaefer M, Hopkins RG, Failla ML, Gitlin JD. Hepatocyte-specific localization and copper-dependent trafficking of the Wilson disease protein in the liver. *Am. J. Physiol.,* **276**, G639-G646, 1999.

Schaefer M, Roelofsen H, Wolters H, Hofmann WJ, Muller M, Kuipers F, Stremmel W, Vonk RJ. Localization of the Wilson disease protein in human liver. *Gastroenterology*, **117**, 1380-1385, 1999.

Scheinberg IH, Sternlieb I. Wilson's Disease in Major Problems in Internal Medicine, Vol. XXIII, W.B. Saunders, Philadelphia, PA.1994

Scheinberg IH, Jaffe ME, Sternlieb I: The use of trintine in preventing the

effects of interrupting penicillamine therapy in Wilson's disease. N *Engl J med* **317**:209-213, 1987.

Walshe JM: Treatment of Wilson's disease with trientine (triethylene tetramine) dihydrochloride. *Lancet* **1**:643-647, 1982.

Schilsky ML: Wilson disease: genetic basis of copper toxicity and natural history. *Semin Liver Dis* **16**:83-95, 1996.

Solioz M, Vulpe C. CPx-type ATPases: a class of P-type ATPases that pump heavy metals. *Trends Biochem Sci* **21**:237-241, 1996.

Sherlock S, dooley J. wilson's disease. In Diseases of the Liver and Biliary Systems, 9th ed. Oxford: Blackwell Scil, pp 400-407, 1993.

Stearman R, Yuan DS, Yamaguchi-Iwai Y, Klausner RD, Dancis A. A permease-oxidase complex involved in high affinity iron uptake in yeast. *Science* **271**:1552-1557, 1996.

Steindl P, ferenci P, Dienes HP, Grimm G, Pabinger I, Madl C, maier-Dobersberger T, Herneth A, Dragostics B, Meyn S, Knoflach P, Granditsh G, gangl A. Wilson's disease in patients presenting with liver disease: A

diagnostic challenge. *Gastroenterology* **113**:212-218, 1997.

Tanzi RE, Petrukhin K, Chernov I, Pellequer JL, Wasco W, Ross B, Romano DM, Parano E, Pavone L, Brzustowicz LM, Devoto M, Peppercorn J, Bush AI, Sternlieb I, Pirastu M, Gusella JF, Evgrafov O, Penchaszadeh GK, Honig B, Edelman IS, Soares MB, Scheinberg IH, Gilliam TC. The Wilson disease gene is a copper transporting ATPase with homology to the Menkes disease gene. *Nat Genet* **5**:344-350, 1993.

Tao TY, Gitlin JD. Hepatic copper metabolism: insights from genetic disease. Hepatology. *Hepatology* **37**:1241-1247, 2003.

Thomas GR, Forbes JR, Roberts EA, Walshe JM, Cox DW. The Wilson disease gene: spectrum of mutations and their consequences. *Nat Genet* **9**:210-217, 1995.

Tsai CH, Wu JY, Chang JG, Lee CC, Lin SP, Yang CF, Jong YJ, Lo MC. Mutation analysis of Wilson disease in Taiwan and description of six new mutations. *Hum Mutat* **12**:370-376,1998.

van De Sluis B, Rothuizen J, Pearson PL, van Oost BA, Wijmenga C.

Identification of a new copper metabolism gene by positional cloning in a purebred dog population. *Hum Mol Genet* **11**:165-173, 2002.

Wilson SAK. Progressive lenticular degeneration: a familial nervous disease associated with cirrhosis of the liver. *Lancet* **1**:1115-1119, 1912.

Wu J, Forbes JR, Chen HS, Cox DW.The LEC rat has a deletion in the copper transporting ATPase gene homologous to the Wilson disease gene. *Nature Genet.* **7**: 541-545, 1994.

Yamaguchi A, Matsuura A, Arashima S, Kikuchi Y, Kikuchi K. Mutations of *ATP7B* gene in Wilson disease in Japan: identification of nine mutations and lack of clear founder effect in a Japanese population. *Hum Mutat Suppl* **1**:S320-322, 1998.

Yamaguchi Y, Heiny ME, Gitlin JD. Isolation and characterization of a human liver cDNA as a candidate gene for Wilson disease. *Biochem Biophys Res Commun* **197**:271-277, 1993.

Yoo HW. Identification of novel mutations and the three most common mutations in the human *ATP7B* gene of Korean patients with Wilson disease. *Genet Med* **4**(6 Suppl):43S-48S, 2002

Yuan DS, Dancis A, Klausner RD. Restriction of copper export in *Saccharomyces cerevisiae* to a late-Golgi or post-Golgi compartment in the secretory pathway. *J Biol Chem* **272**:25787-25793, 1997.

Yuan DS, Stearman R, Dancis A, Dunn T, Beeler T, Klausner RD. The Menkes/Wilson disease gene homologue in yeast provides copper to a ceruloplasmin-like oxidase required for iron uptake. *Proc Natl Acad Sci USA* **92**:2632-2636, 1995.

국문 요약

한국인 윌슨병 환자의 *ATP7B* 유전자 돌연변이 분석 및 기능 연구

윌슨병은 상염색체 열성 질환으로 구리수송에 문제가 발생되어 간과 주변장기에 과도한 구리가 침착되어 일어나는 질병이다. 손상된 구리의 담즙방출과 구리와 세룰로플라즈민의 결합 장애로 인해 윌슨병의 주증상인 간경변과 정신지체를 유발시킨다. *ATP7B* 유전자는 윌슨병의 원인 유전자로써 21개의 엑손과 165kDa의 P형 구리소송 ATPase 단백질을 코딩한다. 한국인의 윌슨병 환자를 대상으로 ATP7B 유전자 돌연변이 검사를 실시하였다. 125명의 혈연관계가 없는 한국인의 윌슨병 환자중에서 30개의 서로 다른 돌연변이를 밝혀냈다 (p.R778L, p.A874V, p.N1270S, c.2513delA, p.T1029I, p.G1035V, p.L1083F, c.2630_2656del, c.2304_2305insC, p.R919G, p.V1106I, p.D1267A, p.C108R, p.E412X, p.C656X, p.M729V, p.R778Q, p.G891D, p.I929V, p.G943S, p.P992L, p.V1024A, p.T1031A, p.C1091Y, p.I1148T, p.A1168S, p.G1186S, p.V1216M, p.P1273L, c.1543+1 G>T). 새롭게 밝힌 돌연변이로 인한 ATP7B 단백질의 기능적 결함을 평가하기 위해, yeast 매개 시스템과 공촛점 현미경을 사용하여 포유동물 세포에 한시적인 발현을 통해 돌연변이들의 단백질 발현 위치를 분석하였다. 5개의 새 돌연변이들은 yeast 발현벡터인 pSY114와

포유동물 발현벡터인 pEGFPC1에 클론하였다. Yeast 매개 시스템에서 p.C656X, p.T1029I, p.T1031A 돌연변이는 단백발현의 이상으로 인해 철 흡수 친화력이 감소되어 yeast의 ccc2 기능을 회복시킬 수 없었다. 이는 ATP7B 단백질의 구리수송 유전자 기능의 결함이 있음을 나타내 주는 결과이다. 임상적으로 증상이 경한 환자인 p.G891D 돌연변이의 단백발현은 yeast의 △ccc2기능을 부분적으로 회복하였다. p.V1106I 돌연변이의 단백발현은 정상인처럼 완벽하게 구리 수송 단백질을 회복시켰다는 점에서 돌연변이라기보다는 다형태라고 판단된다. 공촛점 현미경을 이용한 ATP7B 단백질의 돌연변이 발현 추적 결과, p.C656X 돌연변이의 단백질 발현은 COS-7 숙주세포에서 광범위하게 흩어져 발현되는 양상을 띄었다. p.G891D 돌연변이 단백질은 부분적으로 *trans*-Golgi 부위에서 발현되었다. 그리고 p.T1029I, T1031A 2가지 돌연변이는 주로 핵 주위에서 발현되어 그 주변의 세포 소기관에 잘못 위치하였다. 한편, p.V1106I는 정상적인 ATP7B 단백질 발현 장소와 같은 곳에서 일어났으며, 이러한 결과는 yeast 매개 시스템의 결과와 일치하였다. 윌슨병 환자의 ATP7B 단백질의 기능적인 결함과 유전형-표현형간의 상관관계를 규명하는데 yeast 매개 시스템과 공촛점 현미경 실험결과가 ATP7B 단백질의 기능연구에 유용한 수단으로 이용할 수 있을 것으로 사료된다.

감사의 글

학문의 길을 밟을 수 있도록 돌봐주신 김종배 교수님, 양용석 교수님, 오옥두 교수님, 김태우 교수님, 박용석 교수님, 이혜영 교수님께 깊은 감사의 마음을 드립니다. 학문에 입문할 수 있도록 배려해 주신 서울아산병원 울산의과대학 박인숙 학장님께 감사 드립니다. 의학유전학이란 새로운 분야를 시작할 수 있도록 지도, 편달해주신 서울아산병원 소아과 유한욱 교수님께 진심으로 감사 드립니다. 바쁜 연구업무에도 불구하고 많은 도움을 주신 서을주 선생님, 김영호 선생님께 진심으로 감사 드립니다. 늘 곁에서 함께 하고 격려해주신 김구환 선생님 그리고 유전학클리닉의 많은 선생님들에게 감사 드립니다. 선천성 기형 유전질환 유전체 연구센터를 거쳐간 많은 선생님들과 현재 열심히 일하고 계신 박중영 선생님, 양정윤 연구원, 허선희 연구원, 김주현 연구원, 이진옥 연구원, 고승하 연구원, 이재은 선생님, 그리고 행정업무의 편의를 제공해 주신 김귀주 간호사님과 노은주 씨에게 많은 도움을 받은 점 진심으로 감사 드립니다.

깊이 있는 학문의 길을 갈 수 있도록 독려해주시고 물신양면으로 도와주신 아산생명과학연구소 옛 바이러스 연구실의 우영대 박사님, 김은순 박사님께 진심으로 감사 드립니다. 그리고 저에게 큰 도움을 주셨던 울산의과대학 미생물학교실의 김유겸 교수님께 이 자리를 빌어 감사의 마음을 전하고 싶습니다. 그리고 소중했던 젊은 시절을 함께 동거동락하면서 용기와 자신감을 주었던 변함없는 친구들인 이덕형, 김정한, 강태수, 김재은에게 감사 드립니다. 어려울 때마다 좋은 조언을 아끼지 않은 엄용빈 박사와 지금은 미국에 거주하고 있는 금준섭에게

고마움을 전하고 싶습니다. 이 곳 아산교육연구관에서 같이 근무했던 후배, 승주, 명민, 호중에게도 필요할 때 서슴없이 도와준 점 감사 드립니다. 실험사진 촬영에 도움을 주신 이용진 선생님께도 감사 드립니다. 늘 선배라고 귀찮게 했던 학교 미생물연구실 식구들 규상, 관훈, 승희에게도 감사 드립니다. 서울아산병원 진단검사의학과에 계신 여러 선생님에게도 감사 드립니다. 일본 아키타대학 제1생화학교실의 스기야마, 테라다 선생님께 연구업무에 많은 도움을 주신 점 감사 드립니다. 또한 그 실험실에서 절 보살펴주신 우에노 박사님에게도 감사 드립니다. 이 모든 분들게 감사하다는 말씀 밖에 드릴 말이 없습니다.

늘 청렴하신 아버지와 자상하신 어머니 그리고 항상 좋은 후원자인 두 분 형님과 누님, 형수님들께 옆에서 힘이 되어 주셔서 진심으로 감사 드립니다.

하나뿐인 사위를 늘 따뜻하게 보살펴 주신 장인, 장모님, 항상 긍정적인 사고와 활동적인 처남에게 고마움을 전합니다. 어려웠던 순간순간 저에게 큰 도움을 주신 많은 분들에게 이 자리를 빌어 거듭 감사드립니다. 그리고 그 동안 많은 시간을 집안일에 신경쓰지 못해 힘겨웠던 내 아내에게도 미안함이 앞섭니다. 항상 씩씩한 내 아들 민석이의 눈망울은 저에게 힘을 주기 충분했습니다. 많이 놀아주지 못한 미안함을 이 자리를 빌어 전하고 싶습니다. 이제서야 비로서 사이언스가 무엇인지 조금은 알 것 같습니다. 앞으로는 아름다운 한글로 논문을 쓸 수 있는 시대가 될 수 있도록 조그마한 힘을 보태고자 합니다.